Fusion Loop Modified and Mature Dengue Virus Elicits Protective Serum with Minimal Antibody Dependent Enhancement

Yago R. Dalben[1], Jacob J. Adler[1] Rita M. Meganck[2], Katelyn Duenas[3], Lisa J. Snoderly-Foster[1], Longping V. Tse[1]

[1]Department of Molecular Microbiology and Immunology, Saint Louis University School of Medicine, St. Louis, MO, USA

[2]Department of Molecular Microbiology, Washington University School of Medicine, St. Louis, MO, USA.

[3]MD program Saint Louis University School of Medicine, St. Louis, MO, USA

ABSTRACT

A balanced and safe vaccine against all four-dengue virus (DENV) serotypes is urgently needed. Although the currently licensed DENV vaccines demonstrate efficacy, they also raise concern about vaccine-associated disease enhancement, particularly in DENV-naive individuals. The conserved, immunodominant fusion loop (FL) epitope is the target of cross-reactive, weakly neutralizing antibodies (Abs) which are associated with antibody-dependent enhancement (ADE). Previously, we developed D2-FLM, a highly mature DENV2 strain containing modification in the FL epitope making it unrecognizable to FL-Abs. Here, we grafted the FLM modification to another serotype and adapted them to replicate in Vero cells for live-attenuated vaccine (LAV) manufacturing while retaining favorable antigenic profiles, generating two new strains: D2-vFLM and D4-vFLM. Deep sequencing revealed mutations at the junction of envelope domains I and II (EDI and EDII) that appeared during adaptation of the engineered FL in mammalian cells. Importantly, both D2-vFLM and D4-vFLM showed no evidence of ADE in the presence of FL-targeting Abs. Sera from D2-vFLM immunized mice displayed strong homotypic and reduced heterotypic neutralization compared to wild-type viruses, with minimal to no ADE potential *in vitro*. Moreover, D2-vFLM immunization completely protected AG129 mice from lethal challenge with mouse-adapted D220. Collectively, these findings demonstrate that the FLM modification platform is transferable across serotypes and yields strains with favorable immunogenicity and reduced ADE risk. Our FLM approach provides a promising path toward the development of a safer tetravalent DENV LAV.

INTRODUCTION

Dengue virus (DENV) is the most burdensome human arbovirus, infecting over 50 million people annually[1]. Despite global public health efforts, DENV-related illnesses have steadily increased over the last 75 years, with approximately half of the world's population at risk of DENV infection[2]. Primary DENV infection often leads to asymptomatic or mild disease; however, severe cases of Dengue hemorrhagic fever/Dengue shock syndrome (DHF/DSS) can develop upon secondary infection, causing an estimated 20,000-40,000 deaths annually[1,3]. This unique etiology can be explained by antibody-dependent enhancement (ADE), in which antibodies (Abs) generated from the previous infection cross-react with but do not neutralize the incoming DENV during the next infection, amplifying the severity of the disease[4,5]. Since the first description of DENV ADE in the 1970s, our understanding of its mechanisms remains incomplete[6]. However, accumulating evidence highlights the significant role of weakly neutralizing, cross-reactive antibodies in ADE-mediated infection[7–9]. Unfortunately, there is a mismatch between our lack of understanding of ADE and the growing demographic impact of DENV infection, which is projected to escalate alongside the geographical expansion of the *Aedes* mosquito vectors and the lack of effective preventative measures.

After >20 years of development and clinical trials, three DENV LAVs are at varied phases of clinical approval, but none is recommended for DENV naive populations. The first U.S. Food and Drug Administration (FDA)-approved DENV vaccine, Dengvaxia (3 doses), is recommended for 9-16-year-old adolescents with prior DENV infection, excluding many at-risk populations. DENV naive individuals receiving Dengvaxia showed an increased risk of DENV-related hospitalization compared to placebo groups during clinical trials[10]. The manufacturer, Sanofi, has decided to halt production of Dengvaxia for the US market in 2026. Qdenga (2 doses), a vaccine approved by the European Medicines Agency, voluntarily withdrew its application for FDA approval and, due to low incidence, is unable to provide key clinical trial data addressing vaccine safety concerns in naive individuals infected with DENV3 and DENV4[11,12]. The final candidate in the pipeline, TV005 (single dose), elicits protection against DENV1 and DENV2 in a 2 years follow-up clinical trials[13]. However, conceptually, it is constrained by the same philosophy and technical limitations as its predecessors. It elicits Abs targeting all epitopes, raising similar safety concerns about ADE-prone Abs at later time (> 5 years) after vaccination. Twenty years later, our understanding of ADE has advanced, emphasizing the need to incorporate strategies to minimize ADE-prone Abs into the development of next-generation DENV vaccines to ensure safety and efficacy in naive populations.

The pre-membrane (prM) protein and fusion loop (FL) are epitopes known to be targets of weakly neutralizing, ADE-prone antibodies. PrM shields the FL peptide from premature fusion during egress, while the FL mediates viral membrane fusion with the endosome during entry. The essential functions of prM and FL make them challenging to mutate. Indeed, DENV prM shares approximately 66-80% sequence identity among the four serotypes, while the core 13-amino acid FL is 100% conserved in mosquito-borne orthoflaviviruses. Although prM is normally released after egress, many DENV particles remain partially immature and retain high levels of prM. Methods have been developed to generate mature virions by overexpressing furin protease in producer cells; however, for LAVs, the progeny virus produced in the human body will revert to the immature phenotype. Therefore, current DENV-LAVs present both prM and FL epitopes and elicit strong but potentially undesired antibody responses against them. Supporting this, sera from primary human DENV infections show that a significant proportion of Abs target prM and FL and are weakly neutralizing and ADE-prone, which poses substantial ADE risk for subsequent infections[14]. This issue has been well recognized in vaccine development, and efforts to mask, mutate, or remove prM and FL epitopes have been applied in subunit and mRNA-LNP vaccines[15]. However, such protein-engineering strategies cannot be directly translated to LAVs, where these elements are required for viral function.

The highly effective flavivirus vaccine against Yellow Fever virus, Y17D[16], as well as all licensed DENV vaccines are LAVs[17]. LAVs mimic natural infection and elicit strong humoral and cell-mediated responses against both structural and non-structural proteins. Importantly, unlike other vaccine platforms which requires multiple boosters, TV005 (the most advanced DENV-LAV) provides protection with a single dose[18], a critical feature for low-income regions where multi-dose regimens are difficult and where partial immunity between doses may increase the risk of ADE.

Previously, our group reported genetically modified mature DENV and a FL-mutated, fully mature DENV2 (D2-FLM) that is insensitive to FL- and prM-targeting Abs[19]. In this study, we extended this strategy by grafting the FLM mutations onto a genetically distinct serotype (DENV4) and adapting both FLM viruses in Vero cells to generate D2- and D4-vFLM, suitable for large-scale LAV manufacturing. Both vFLM strains retained their intended antigenic properties and did not cause ADE in the presence of FL-Abs. Immunization with D2-vFLM elicited robust neutralizing antibody responses against the homotypic virus and, to a lesser extent, the heterotypic virus. Importantly, immune sera from D2-vFLM viruses show minimal ADE activity *in vitro*. Furthermore, AG129 mice immunized with D2-vFLM were fully protected against lethal challenge with mouse-adapted D220. Together, these findings suggest that the FLM mutations represent a promising

99 and potentially safer LAV platform, capable of generating favorable humoral responses to protect
100 DENV-naïve individuals while minimizing vaccine-related ADE.
101

102 **RESULTS**

103 Generation and characterization of Vero-adapted D2-vFLM

104 All currently licensed or advanced DENV LAVs are manufactured in Vero cells[20,21]. Thus,
105 the ability to replicate in this cell line is a critical requirement for further development of the FLM
106 series as a potential LAV candidate. As we previously reported, D2-FLM strain replicates to levels
107 comparable to isogenic DV2 in C6/36 cells[19]. However, D2-FLM is attenuated in Vero cells; in
108 multi-cycle growth curves, no detectable titer was measured in over five days. To understand the
109 growth defect, we performed immunostaining with anti-NS3 antibody at 24hpi. Robust NS3
110 staining was detected in DV2 infected cells, but no signal was observed in D2-FLM infected cells,
111 suggesting that the block occurs early in infection, prior to NS3 translation **(Fig. 1A)**.

112 Because C6/36 cells are cultured at 32°C whereas Vero cells are maintained at 37°C, we
113 hypothesized that D2-FLM might be temperature sensitive. To test this, Vero cells were infected
114 with DV2 or D2-FLM (MOI = 0.05) and incubated for five days at either 32°C or 37°C. Infectivity
115 was assessed by immunostaining for prM and E proteins at day 5 post-infection. DV2 showed
116 robust staining at both temperatures, with nearly complete infection across the well. In contrast,
117 D2-FLM exhibited moderate staining at 32°C with scattered foci but showed no evidence of
118 replication at 37°C **(Fig. 1B)**. These findings indicate that D2-FLM is partially temperature
119 sensitive and that 32°C is permissive for low-level replication in Vero cells, allowing for
120 experimental tissue-culture adaptation. To achieve this, D2-FLM was serially passaged on Vero
121 cells at 32°C for 3–5 passages to promote mammalian cell adaptation, followed by an additional
122 3–5 passages at 37°C for temperature adaptation **(Fig. 1C)**. Infectivity, assessed by prM and E
123 staining, increased progressively with passage number (data not shown). After the final passage,
124 we collected the adapted virus and designated it D2-vFLM, where "v" indicates Vero-adapted.

125 D2-vFLM replicates in Vero cells at 37°C, reaching peak titers of ~4× 10^5 FFU/mL at day
126 3 post infection **(Fig. 1D)**. Notably, D2-vFLM remained mildly attenuated, with a 10-fold reduction
127 in peak titer compared with DV2 (~3×10^6 FFU/mL; **Fig. 1D)**. In C6/36 cells, D2-vFLM grows with
128 similar kinetics to D2-FLM, reaching ~5x10^6 FFU/ml at 3dpi, while DV2 reaches peak titers of
129 1x10^7 FFU/mL at 5dpi **(Fig. 1E)**. The maturation phenotype of D2-FLM is generated by the
130 genetically modified furin cleavage site in prM[22]. As expected, western blot analysis confirmed
131 that D2-vFLM retains the highly mature virion phenotype **(Fig. 1F)** with an 80% reduction of
132 unprocessed prM compared to DV2 in normal Vero-81 producer cells **(Fig. 1G)**.

133 To assess virion stability, we performed an infectivity assay using nano-luciferase (nLuc)
134 reporter DENV. D2-vFLM-nLuc was rederived by reverse genetics and incubated at temperatures
135 from 4°C to 55°C and pH levels from 5.4 to 8.4. Infectivity was normalized to untreated controls

136 and compared with DV2. Interestingly, DV2 displayed up to a 2.5-fold increase in infectivity after
137 incubation at temperatures from 32-42°C. In contrast, D2-vFLM infectivity was stable from 4-37°C,
138 with a noticeable decrease beginning at 42°C. As expected, treatment at 55°C completely
139 inactivated both D2-vFLM and DV2 **(Fig. S1A)**. Although some variation was observed between
140 experiments, D2-vFLM displayed similar pH stability to DV2 from pH 5.4 to pH 8.4. At acidic pH,
141 a 20–40% loss of infectivity was observed for both viruses **(Fig. S1B)**. These results suggest that
142 the thermostability and pH stability of D2-vFLM are similar to wild-type viruses.

143 Mutations in the structural protein are selected for during Vero adaptation.

144 To confirm the stability of FLM modifications and to identify compensatory mutations after
145 Vero adaptation, we deep sequenced the D2-vFLM virus. First, the FLM mutations are stable and
146 do not revert to the wild-type sequence after eight passages. Second, we identified a total of six
147 fixed mutations in both the structural and non-structural genes, including prM-E18D, Env-P53T,
148 Env-T171A, Env-K204R, NS2A-L181F, and NS4b-L112F **(Table 1)**. To determine which mutations
149 were driving adaptation, we generated two variants: D2-vFLM-structural and D2-vFLM-
150 nonstructural, which carried only the structural or non-structural adaptation mutations,
151 respectively. Individual genome fragments containing the desired mutations were cloned, and
152 infectious clones were recovered in C6/36 cells using reverse genetics **(Fig. 2A)**. Working stocks
153 were subsequently prepared by propagation in either C6/36 cells (insect-grown) or Vero cells
154 (mammalian-grown). Deep sequencing of all stocks confirmed the presence of the core FLM
155 mutations and the intended adaptation mutations **(Table 1)**.

156 For D2-vFLM-structural, the mammalian-grown stock contained three spontaneous
157 mutations at low frequency: NS1-M89V (31%), NS3-D409E (14%) and NS4b-V115A (13%) **(Table**
158 **1)**. In contrast, sequencing of the mammalian-grown D2-vFLM-nonstructural stock revealed three
159 structural mutations at >95% frequency: prM-L41V, Env-T171A (present in the original D2-vFLM),
160 and T404K, yielding a virus with the intended non-structural changes plus three additional
161 structural changes **(Table 1)**. These findings suggest that structural protein mutations are strongly
162 favored to co-evolve with FLM mutations in mammalian cells.

163 To assess replication kinetics, we performed multi-cycle growth curve experiments with
164 mammalian-grown D2-vFLM-structural and D2-vFLM-nonstructural viruses in Vero cells. D2-
165 vFLM-structural exhibited growth kinetics similar to D2-vFLM, reaching peak titers of ~3×10^5
166 FFU/mL at 3 dpi. In contrast, replication of D2-vFLM-nonstructural was slower, peaking at 5 dpi
167 **(Fig. 2B)**. Interestingly, when insect-grown virus stocks were used for Vero-81 growth curves,
168 both D2-vFLM-structural and -nonstructural viruses showed a 48h delay in replication, and viral
169 titer did not exceed 10^5 FFU/mL after 5 days **(Fig. 2C)**. These data indicate that C6/36-grown

170 D2-vFLM displays non-genetic attenuation in mammalian cells, providing an added safety feature
171 of the LAV by reducing the risk of insect-to-human transmission.

172 FLM mutations can be directly grafted onto DENV-4

173 We envision the FLM mutations as platform technology for developing a tetravalent DENV
174 LAV. As a proof-of-concept, we examined the compatibility of the FLM mutations in the most
175 genetically distinct serotype, DENV4. The core FLM mutations were introduced into a DENV4-Sri
176 Lanka 1992 backbone and a viable virus was successfully recovered in C6/36 cells using reverse
177 genetics. Multi-cycle growth curve analysis of D4-FLM on Vero cells revealed a strong attenuation
178 phenotype like D2-FLM. D4-FLM showed a >2-log reduction in peak titer (~10^4 FFU/mL)
179 compared to the isogenic DV4 control (~10^6-10^7 FFU/mL) at 4dpi **(Fig. 3A)**. These findings
180 indicate that FLM mutations are transferable to other DENV serotypes and have a predictable
181 attenuation on Vero cell replication.

182 To overcome this growth defect, we subjected D4-FLM to serial passage in Vero cells at
183 37°C for four rounds, similar to the approach used with D2-FLM. The adapted virus, termed D4-
184 vFLM, regained replication capacity comparable to wild-type DENV4, reaching titers of ~10^6-10^7
185 FFU/mL by d4pi **(Fig. 3A)**. Deep sequencing confirmed retention of the FLM mutations, along with
186 additional adaptive mutations in structural proteins: prM-K52E (97.4%), Env-F193Y (97.5%), and
187 Env-E417A (100%). No mutations were identified in non-structural proteins **(Fig. 3B)**. Although
188 no overlapping adaptive mutations were identified between D2-vFLM and D4-vFLM, structural
189 adaptations were concentrated at the EDI and EDII junction of the envelope protein **(Fig. 3C)**,
190 suggesting a possible structural hotspot for FL mutations compensation.

191 Antigenic properties of D2- and D4-vFLM.

192 We previously demonstrated that D2-FLM exhibits distinct antigenic properties, becoming
193 insensitive to FL-targeting antibodies (FL-Abs). However, there was a possibility that additional
194 structural mutations in D2-vFLM might alter these unique antigenic features. To address this, we
195 performed foci reduction neutralization titer (FRNT) assays on Vero cells testing D2-vFLM and
196 D4-vFLM against a panel of monoclonal antibodies. Consistent with earlier findings, $FRNT_{50}$
197 values for non-FL antibodies, including prM (2H2, non-neutralizing), EDE antibodies (EDE1-C10
198 and EDE2-B7), EDIII antibody (2D22), and EDI antibody (3F9), showed no significant differences
199 between D2-vFLM and DV2. In contrast, D2-vFLM displayed varying degrees of reduced
200 sensitivity to FL-Abs (1M7, 1L6, and 4G2) compared to DV2 **(Fig. 4B)**. Similarly, D4-vFLM
201 exhibited altered antigenicity, with selective loss of sensitivity to FL-Abs (1M7, 1L6, and 4G2)
202 while remaining minimally affected by broadly neutralizing EDE antibodies (EDE1-C10 and EDE2-
203 B7) **(Fig. 4B)**.

204 To facilitate future studies, we generated D2-vFLM-nLuc and D4-vFLM-nLuc reporter
205 viruses using reverse genetics based on the design reported previously. Neutralization assays
206 with these reporter viruses yielded EC_{50} values that were consistently ~10-fold lower (more
207 sensitive) than $FRNT_{50}$ values across multiple antibodies **(Fig. 4C and 4D)**, though the relative
208 potency remained largely unchanged. One notable exception was observed with D4-vFLM-nLuc
209 against 1M7: the nLuc EC_{50} (~0.05 μg/ml) was comparable to DV4, whereas the $FRNT_{50}$ of D4-
210 vFLM was significantly higher (~2.78 μg/ml) **(Fig. 4D)**. This discrepancy is not readily explained;
211 however, deep sequencing revealed a unique mutation (prM-E89S) in D4-vFLM-nLuc, while D4-
212 vFLM carried prM-K52E. These differences may provide testable hypotheses for future
213 investigation but are beyond the scope of the present study.

214 Immunization with D2-vFLM generates neutralizing serum comparable to DV2

215 To compare the immunogenicity of the D2-vFLM virus with wild-type DV2, we immunized
216 3-4-month-old C57BL/6 mice (both male and female) via intramuscular (I.M.) injection in the hind
217 leg with $2.5x10^5$ FFU of DV2 (n=10) or D2-vFLM (n=11) adjuvanted with AddaVax. A relatively
218 high dose was chosen compared with the human (human dosage: 10^3-10^5 PFU per dose) due to
219 the inability of DENV to replicate efficiently in immunocompetent mice. Mice received three
220 immunizations as prime/1°boost/2°boost administered at two-week intervals. Homotypic and
221 heterotypic serum neutralization titers were measured using our nLuc-based neutralization assay.
222 Pooled serum from pre-immunization, after prime, after 1°boost, and after 2°boost shows steady
223 increase in neutralization titer **(Fig. 5A;** individual neutralization curves in **Fig. S2)**. Robust
224 seroconversion started after 1°boost and peaked after 2°boost. Homotypic EC_{50} against DENV2
225 reaches ~1:1000 for both viruses. Heterotypic EC_{50} against DENV4 were minimal and only
226 appears after 2°boost.

227 To gain better understanding of seroconversion of individual animals, we perform
228 neutralization assay on each serum after 2°boost. EC_{50} valves span over a 10-fold range, from
229 1:300 to 1:3000 while the mean EC_{50} values against homotypic DENV2 were ~1:1000 for DV2
230 and 1:800 for D2-vFLM; against the heterotypic DENV4, mean EC_{50} values were 1:180 and 1:110,
231 respectively **(Fig. 5B;** individual neutralization curves in **Fig. S3A and S3B)**. Our data suggests
232 that the FLM mutations in D2-vFLM may modestly reduce immunogenicity, potentially due to the
233 loss of immunodominant epitopes, although this difference did not reach statistical significance.
234 Overall, D2-vFLM viruses elicited neutralizing antibody responses comparable to those induced
235 by DV2.

236 Serum from D2-vFLM shows minimal to no ADE responses against heterotypic viruses

237 To compare the heterotypic ADE potency of D2-vFLM and DV2 serum, we developed a
238 high-throughput nLuc-based ADE assay. In our assay, we evaluated three antibodies targeting
239 distinct antigenic regions, including 4G2 (FL-Ab), 2H2 (prM-Ab), and B7 (EDE-Ab), using DV4-
240 nLuc reporter viruses on K562 cells. As expected, all three antibodies enhanced DV4-nLuc
241 infection at peak dilution/concentrations of 1:100 (4G2 hybridoma) **(Fig. 6A)**, 1:100 (2H2
242 hybridoma) **(Fig. 6B)**, and 1 µg/ml (B7) **(Fig. 6C)**. In contrast, 4G2 did not enhance infectivity of
243 D4-vFLM, while 2H2 induced only a modest level of enhancement. Because the EDE epitope is
244 preserved in the vFLM viruses, D4-vFLM exhibited similar peak ADE concentrations for B7
245 compared to DV4 **(Fig. 6C)**. We benchmarked our results against published data obtained using
246 conventional flow cytometry-based ADE assays and flaviviral single-round infectious particle
247 (SRIP) systems. Results from published ADE assays can be variable; however, our results fall
248 within the reported range in both fold-increase (10–100-fold) and antibody concentration (0.1–5
249 µg/ml 4G2-Ab) for enhancement[23–25]. These data validate our nLuc-based ADE assay, and that
250 the FLM mutations render DENV inert to ADE mediated by FL-Abs.
251 Based on the neutralization assay, we analyze the ADE potency of 2°boost serum of DV2
252 (n=5) and D2-vFLM (n=4) that are positive against heterotypic DV4. Pooled, positive sera from
253 DV2-immunized mice against the heterotypic DV4-nLuc exhibited approximately 75-fold increase
254 at peak compared to no serum control **(Fig. 6D)**. In contrast, pooled, positive D2-vFLM-immunized
255 sera exhibited negligible ADE. Additionally, DV2-immunized sera did not enhance D4-vFLM-nLuc
256 infection, further support that the enhancing Abs in the polyclonal serum target FL- and prM-
257 epitopes **(Fig. 6D)**. Overall, our data demonstrates that FLM modifications achieve a key
258 immunological objective by minimizing heterotypic ADE. Full neutralization and ADE curves of
259 individual serum samples can be found in supplementary figure 4 **(Fig. S4)**.
260 <u>D2-vFLM immunization protects mice from lethal challenge in AG129 mice</u>
261 To test *in vivo* protection, male and female AG129 mice (4-6-months-old) were immunized
262 with DV2 (n=4, one animal died before challenge); D2-vFLM (n=5); or mock immunized (n=6, one
263 animal died before challenge) with the same dosing regimen as above. Three weeks after the
264 final boost, mice were challenged with $5x10^5$ FFU of mouse-adapted D220 via tail-vein
265 intravenous (I.V.) injection following published protocols[26]. In mock immunized mice, weight loss
266 was observed beginning at 2dpi**,** and lethality at 5dpi, reaching 83% mortality by 10dpi **(Fig. 7A**
267 **and 7B)**. Viral titers were detected in sera from mock immunized mice, peaking at $6.2x10^6$ FFU/ml
268 on d3pi **(Fig. 7C)**. D2-vFLM immunized mice showed complete protection from weight loss, viral
269 titer (limit of detection: 200 FFU/ml), and death, similar to DV2 immunized mice **(Fig. 7)**. Our data
270 demonstrates D2-vFLM immunization can protect from homotypic infection *in vivo*.

271 **DISCUSSION**

272 Antibodies targeting the FL- and prM-epitopes have been associated with ADE[8,9].
273 Therefore, Dengue and flavivirus vaccine design strategies often aim to mask or eliminate the FL
274 epitopes[15,27–29]. However, the requirement for a fully functional FL in the LAV platform has posed
275 a significant challenge for the development of a FL-modified DENV-LAV[30]. Previously, using
276 directed evolution, we introduced mutations in the FL and showed that the resulting virus, D2-
277 FLM, exhibited the intended antigenic property of reduced recognition by FL-targeting
278 antibodies[19]. However, these mutations also resulted in the inability of D2-FLM to grow in Vero-
279 81 cells, the production cells for DENV-LAV manufacturing. In this study, we extended our
280 previous work by adapting the FLM virus to enable growth in Vero cells and generating two Vero-
281 adapted FLM viruses, D2-vFLM and D4-vFLM, and evaluating D2-vFLM potential as LAV
282 candidates.

283 D2- and D4-vFLM both grow in Vero-81 cells, supporting FLM modifications can be
284 transfer to other DENV serotypes as well as orthoflaviviruses for direct downstream vaccine
285 manufacturing. Like the parental FLM viruses, vFLM strains have lost or reduced neutralization
286 and enhancement by FL-targeting antibodies. Mice immunized with D2-vFLM seroconverted and
287 showed neutralization potency comparable to their WT counterparts. Although we did not
288 compare the cell-mediated responses between D2-vFLM and DV2, we expect the mutations of
289 the vFLM virus would have minimal effect on T-cell epitopes as most of the CD4 and CD8 epitopes
290 are from non-structural proteins, such as NS3[31,32]. Importantly, using an *in vitro* ADE assay, our
291 data indicates that D2-vFLM induces qualitatively different antibody responses that do *not*
292 enhance heterotypic infection. *In vivo* protection was evaluated in a homotypic format and D2-
293 vFLM immunized AG129 mice were completely protected from mouse-adapted D220 challenge.
294 Overall, DENV strains carrying FLM modifications elicited a safer antibody profile while
295 maintaining immunogenicity in mice, a critical step to improve the safety of DENV-LAV.

296 Because the FLM mutations are deleterious to viral replication in Vero-81 cells,
297 compensatory mutations were required to restore fitness. We did not identify consensus
298 compensatory mutations between different serotypes, but they are primarily located in the hinge
299 region between EDI and EDII. A plausible hypothesis is that the FLM modifications may influence
300 the conformational transition between the pre-fusion dimeric and post-fusion trimeric forms that
301 are only affected in mammalian cells[33,34]. We are currently investigating this phenomenon to
302 identify universal compensatory mutations that could eliminate the need for adaptation of
303 additional strains.

304 The generation of FLM viruses not only holds potential for incorporation into next-
305 generation DENV-LAVs to improve safety but also provides valuable tools for characterizing anti-
306 DENV sera. Owing to their unique antigenicity, which reduces recognition by FL- and prM-
307 targeting antibodies, FLM viruses can be used to determine neutralizing antibodies in serum
308 without the influence of weakly neutralizing FL- and prM-Abs (a better representation for type
309 specific neutralizing potency)[35] and as an antigen for serum depletion[36,37]. Importantly, our *in vitro*
310 ADE assays clearly, and perhaps is the first time to directly demonstrate that FL-targeting
311 antibodies are the main contributors to ADE in polyclonal serum. Therefore, generating FLM
312 variants for all DENV serotypes will enable the targeted separation of weakly neutralizing
313 antibodies from other antibody populations in complex polyclonal sera, providing an extra
314 dimension for assessing serum quality and vaccine assessment.
315 In this study, we developed an nLuc-based ADE assay to improve throughput. As with
316 other *in vitro* ADE assays, the magnitude of enhancement reported as fold-change (nLuc) or
317 percentage of infected cells (flow cytometry) is inherently variable and can be influenced by
318 multiple factors including expression level of CD32a on K562 cells (in human CD16a)[38], baseline
319 nLuc signal, and virus maturity or stability. To ensure data quality and plate-to-plate consistency,
320 internal monoclonal antibody standards (4G2 and B7) were included on every assay plate.
321 Although absolute enhancement values should not be overinterpreted, the ranges of antibody or
322 serum concentrations that produce enhancement were highly consistent. Importantly, peak ADE
323 concentrations should be evaluated alongside neutralization titers (EC_{50}) to interpret the biological
324 properties of a serum or antibody. Nevertheless, serum from D2-vFLM-immunized mice displayed
325 clear heterotypic neutralization against DV4 but did not exhibit measurable ADE, indicating that
326 these cross-reactive antibodies are non-enhancing. These antibodies may represent EDE-type
327 responses or a distinct class of cross-reactive antibodies with minimal enhancement capacity. We
328 are currently working to define the specificity of these antibodies.
329 Not all FL-targeting antibodies are weakly neutralizing, and some protective antibodies
330 have overlapping footprints on the FL epitopes. Compared with other reported mutations in the
331 FL region of flavivirus vaccine candidates, the N103S and G106L substitutions described here
332 are relatively conservative, which may explain their retained functionality. This is important not
333 only for LAV development but also for maintaining the overall immunogenicity of the vaccine. As
334 shown in our neutralization data, both D2-vFLM and D4-vFLM remain sensitive to neutralization
335 by EDE1-C10, a cross-reactive quaternary antibody with a limited footprint on the FL. Functionally
336 preserving the FL may also help maintain the structural integrity of the FL region, thereby retaining
337 epitopes recognized by other protective antibodies that partially overlap with the FL[39].

338 Despite the negative perception surrounding the current DENV vaccines, all licensed
339 formulations have been shown to be safe and protective in DENV-experienced populations,
340 saving thousands of lives. Nevertheless, there remains room for further improvement in safety for
341 DENV-naïve populations. Here, we report a targeted approach to enhance the safety of DENV-
342 LAV. We also suggest that our FL mutations preserve the structure and function and may also
343 have implications for other emerging vaccine platforms such as mRNA-LNP, E-dimer, and virus-
344 like particle (VLP) vaccines. The transferability of the FLM modification to other DENV serotypes
345 also enables rapid engineering of new strains and other orthoflaviviruses to address potential
346 breakthrough infections caused by diverse DENV genotypes[40,41]. LAVs mimic natural infection,
347 generating robust humoral and cell-mediated immune responses. They also represent the most
348 practical and economical vaccine platform, capable of providing protection with a single dose in
349 DENV endemic regions. To date, LAVs remain the only proven vaccine platform in clinical use
350 with demonstrated efficacy against DENV infection. However, as history has shown,
351 indiscriminately chasing immunogenicity of DENV vaccines can be risky especially when the ADE-
352 prone FL-epitope is also immunodominant[14,42]. It is therefore our responsibility to ensure that
353 future vaccine designs continue to balance both efficacy and safety for all populations.

354 **MATERIALS AND METHODS**

355 **Cells and Viruses**

356 *Aedes albopictus* C6/36 cells (ATCC CRL-1660) were cultured in MEM (Gibco)
357 supplemented with 5% FBS (HyClone), 1% penicillin/streptomycin (Gibco), 0.1 mM nonessential
358 amino acids (Gibco), 1% HEPES (Gibco), and 2 mM GlutaMAX (Gibco) at 32°C with 5% CO_2.
359 African green monkey Vero-81 cells (ATCC CCL-81) were maintained in DMEM/F12 (Gibco)
360 supplemented with 10% FBS, 1% penicillin/streptomycin (Gibco), 0.1 mM nonessential amino
361 acids (Gibco), and 1% HEPES (Gibco) at 37°C with 5% CO_2. K562 cells were cultured in
362 suspension in RPMI-1640 medium (Sigma-Aldrich) supplemented with 10% fetal calf serum
363 (Cytiva), 2 mM L-glutamine, and 1% penicillin–streptomycin (Sigma-Aldrich) at 37°C in a
364 humidified atmosphere containing 5% CO_2. The medium was renewed every 2-3 days by adding
365 or replacing fresh complete medium. DENV viruses (DV2-S16803, GenBank accession:
366 GU289914; DV4-SriLanka-92, GenBank accession: KJ60504.1) were propagated in either C6/36
367 or Vero-81 cells using infection media. C6/36 infection media consisted of Opti-MEM (Gibco)
368 supplemented with 2% FBS (HyClone), 1% penicillin/streptomycin (Gibco), 0.1 mM nonessential
369 amino acids (Gibco), 1% HEPES (Gibco), and 2 mM GlutaMAX (Gibco). Vero-81 infection media
370 consisted of DMEM/F12 (Gibco) supplemented with 2% FBS, 1% penicillin/streptomycin (Gibco),
371 0.1 mM nonessential amino acids (Gibco), and 1% HEPES (Gibco). D2-vFLM was adapted from
372 previously described D2-FLM[19] through 5 passages on Vero-81 at 32°C, followed by 5 passages
373 on the same cell line at 37°C. Dengue nLuc reporter viruses were created using a four-plasmid
374 system in which nLuc reporter was inserted into the viral genome as previously described[43]. In
375 short, nLuc gene was cloned after the coding sequence of the first 38 amino acids of the DENV
376 capsid gene, linked by the Thosea asigna virus 2A (T2A) self-cleaving peptide. Additionally, a
377 codon-optimized C38 sequence was placed after T2A to prevent homologous recombination
378 between the two C38 sequences. Stock viruses are deep-sequenced in-house using a iSeq100
379 platform with 500x - 1000x genome coverage.

380 **DENV focus-forming assay**

381 Virus titers were determined using a focus-forming assay in a 96-well plate. Vero-81 and
382 C6/36 cells were seeded at densities of $2x10^4$ and $1x10^5$ cells per well, respectively, one day
383 before infection. The following day, virus was serially diluted 10-fold across eight dilutions, and 50
384 µL of each dilution was added to wells after removing the growth medium. The plate was
385 incubated for 1 hour at 37°C (Vero-81) or 32°C (C6/36). Post-incubation, 125 µL of overlay
386 medium (Opti-MEM supplemented with 2% FBS, 1% NEAA, 1% P/S, and 1% methylcellulose)
387 was added to each well, and infection proceeded for 48 hours. The overlay was then removed,

388 and wells were washed three times with PBS before fixation with 10% formalin in PBS for 30
389 minutes. Cells were blocked using a permeabilization buffer (ThermoFisher, 00-8333-56)
390 containing 5% non-fat dried milk. Primary antibodies, anti-prM 2H2 and anti-E 4G2 (from non-
391 purified hybridoma supernatant), were diluted 1:200 in blocking buffer, and 50 µL of the diluted
392 primary antibody was added to each well. The plate was then incubated at 37°C for 1 hour. After
393 incubation, wells were washed before adding 50 µL of a goat anti-mouse HRP secondary antibody
394 (SeraCare KPL 54500011) diluted 1:2,000. The plate was incubated at room temperature for 1
395 hour, followed by additional washing steps. Foci were then stained using TrueBlue HRP substrate
396 (SeraCare) and quantified with an ImmunoSpot analyzer (Cellular Technology).

397 **DENV infectivity assay using nLuc-reporter viruses**

398 One day before infection, Vero-81 cells were seeded at $2x10^4$ cells per well in a black 96-
399 well plate (Corning Costar). After 24 hours, the virus was serially diluted 10-fold across eight
400 dilutions. The growth medium was removed from the cell plate, and 50 µL of each dilution was
401 added to the corresponding wells. The plate was then incubated at 37°C for 48 hours. Following
402 incubation, Nano-Glo Luciferase Assay substrate (Promega) was added to each well, following
403 manufacturer's protocol, and luciferase activity was detected using GloMax Plate Reader
404 (Promega) as surrogates for viral infection.

405 **DENV maturation via western blot**

406 Viral supernatants were mixed with 4x Laemmli Sample Buffer (Bio-Rad) and heated at
407 95°C for 5 minutes. Proteins were separated through SDS-PAGE electrophoresis, transferred to
408 a PVDF membrane, and blocked with 5% nonfat milk in TBS-T. The membrane was incubated for
409 1 hour at 37°C with polyclonal rabbit anti-prM (1:1,000; Invitrogen PA5-34966) and polyclonal
410 rabbit anti-Env (1:1,000; Invitrogen PA5-32246) in 2% BSA in PBS-T. After incubation, membrane
411 was thoroughly washed with TBS-T and incubated for 1 hour at room temperature with goat anti-
412 rabbit HRP (1:10,000; Jackson ImmunoLab) in 5% milk in TBS-T. Detection was performed using
413 SuperSignal West Pico Plus chemiluminescent substrate (ThermoFisher), and imaging was
414 carried out on ChemiDoc Imaging system (Bio-Rad). Band pixel intensity was quantified using
415 Image Lab software (Bio-Rad), and relative maturation was determined using the equation:
416 (prMExp/EnvExp)/(prMWT/EnvWT).

417 **DENV Growth Kinetics**

418 Vero-81 and C6/36 cells were seeded on 6-well plates one day before infection, at a
419 concentration of $4x10^5$ and $5x10^5$, respectively. Cells were infected with an MOI of 0.05-0.1,
420 estimating $8x10^5$ (Vero-81) and $1x10^6$ (C6/36) cells on the day of infection. After virus was added
421 to the cells, plates were incubated for 1 hour at 37°C (Vero-81) or 32°C (C6/36), followed by 3x

422 washes with PBS and replenishment with fresh infection medium. At 0, 24, 48, 72, 96, and 120
423 hours after infection, 300 µL of viral supernatant was collected, followed by replenishing with the
424 same amount of fresh infection media, and stored at -80°C. Dengue focus-forming assay was
425 performed, as previously described, for each time point. All experiments were performed
426 independently at least three times.

427 **Thermostability and pH stability assays**

428 Viruses were thawed and incubated at 4°C, 32°C, 37°C, 42°C and 55°C for 1 hour,
429 followed by virus quantification luciferase reporter assay, as previously described. All experiments
430 were performed independently at least three times. For pH stability assay, we prepare infection
431 medium adjusted at 4 different pH (5.4, 6.4, 7.4, and 8.4) using hydrochloric acid or sodium
432 hydroxide. Viruses were mixed 1:1 with the pH-adjusted media and incubated for 1 hour at 4°C.
433 Following incubation, virus quantification was performed using luciferase reporter assay, as
434 previously described. All experiments were performed independently at least three times.

435 **Focus reduction and nLuc based-neutralization titer assays**

436 Focus reduction neutralization titer (FRNT) assays were conducted as previously
437 described. One day prior infection, $2x10^4$ Vero-81 cells were seeded in a 96-well plate. Antibodies
438 were serially diluted and mixed with the DENV at 100 FFU/well (FRNT) or DENV-nLuc at 800
439 FFU/well (nLuc-based) at a 1:1 ratio and incubated for 1 hour. The mixture was then added to the
440 cells and incubated for another hour before applying the overlay (Opti-MEM supplemented with
441 2% FBS, 1% NEAA, 1% P/S, and 1% methylcellulose). Plates were incubated for 48 hours, after
442 which viral foci were stained and counted, as previously detailed in 'DENV focus-forming assay'
443 or Nano-Glo Luciferase Assay substrate was added for the nLuc-based assay. The neutralization
444 % is fitted to a variable slope sigmoidal dose-response curve, using GraphPad Prism 10. For
445 serum neutralization, $FRNT_{50}$ values were determined from an eight-point dilution curve starting
446 at 1:40, followed by 4-fold serial dilutions. All experiments were performed independently at least
447 three times.

448 **ADE assay using nLuc-reporter DENV**

449 Antibody-dependent enhancement (ADE) was evaluated using K562 cells cultured in
450 suspension. On day -1, K562 cells were seeded at $>1x10^6$ cells/mL. On the day of experiment,
451 cells were counted and seeded into black, flat-bottom 96-well plates at a density of $1x10^5$ cells
452 per well. Ab or serum samples were serially diluted at four-fold interval for eight times in infection
453 medium (RPMI-1640 supplemented with 2% fetal bovine serum and 1% penicillin–streptomycin),
454 with starting dilution of 1:80. The virus was diluted in the same medium to achieve 5,000 focus-
455 forming units (FFU) per well. Equal volumes of diluted serum and virus (25 µL each) were mixed

456 and incubated at 37°C for 1h and added to the plated cells (50 µL per well), resulting in a total
457 volume of 100 µL per well. Each plate included a negative control consisting of K562 cells infected
458 with virus only, which served as a baseline for normalization and two mAb (4G2 and B7)
459 standards. Plates were incubated for 24 hours at 37°C in a humidified 5% CO_2 incubator.
460 Following incubation, the Nano-Glo Luciferase Assay substrate (Promega) was prepared
461 according to the manufacturer's instructions and added directly to each well. Luminescence was
462 measured using a NanoGlo luciferase reader (Promega), and results were reported as fold-
463 change compared to no Ab control.

464 **Next Generation Sequencing**

465 Viral RNA was isolated using TRIzo LS (Invitrogen), following the manufacture's protocol.
466 Samples for next generation sequencing (NGS) library were generated via Click-seq protocol
467 based on previously described work-flow[44]. In brief, reverse transcription was carried out using
468 Superscript IV Reverse Transcriptase (Invitrogen) according to the manufacturer's protocol,
469 except that the reaction was supplemented with small amounts of azido-nucleotides (AzNTPs).
470 ClickSeq was carried out for library preparation, incorporating Illumina TrueSeq Index Primers.
471 Libraries were quantified using Quantus Fluorometer (Promega) and sequenced using Illumina
472 iSeq 100 System with a pair-ended 150bp x 2 reagents. Each sample was aimed for 100x genome
473 coverage with final coverage after QC ranging from 500x – 1000x. Raw fastq files were imported
474 to Geneious Prime software for quality control and variant calling after aligned to the original viral
475 genome.

476 **Mouse immunization**

477 Male and female C57BL/6 (B6) mice, 3-4 months of age, were used for immunizations.
478 Animals were randomly assigned to receive either the DV2 or D2-vFLM viruses, with each group
479 consisting of 10 - 11 animals. Each mice received 2.5×10^5 FFU DENV2 in PBS and mixed with an
480 equal volume of AddaVax adjuvant (InvivoGen). Immunizations were delivered intramuscularly
481 into the hind leg. The schedule consisted of a prime immunization, followed by a first boost two
482 weeks later and a second boost two weeks after the first boost. Blood samples were collected
483 prior to each immunization by submandibular bleed using BD Microtainer SST gel tubes. Two
484 weeks after the second boost, mice were euthanized, and blood was obtained by cardiac
485 puncture. Samples were allowed to clot at room temperature and serum were collected after low-
486 speed centrifugation. The resulting serum was transferred to 1.5 mL microcentrifuge tubes and
487 heat-inactivated at 55 °C for 30 minutes before storage and further analysis.
488
489

490 **AG129 challenge model**

491 Male and female AG129 mice, 4-6 months-old were immunized with $5x10^4$ FFU of DV2,
492 D2-vFLM or mock with AddaVax (3:1) immunized with the same route and schedule as described
493 above. Three weeks after the final boost, mice were infected with $5x10^5$ FFU of mouse-adapted
494 D220 via tail-vein intravenous (I.V.) injection in PBS. Body weights were measured daily for 10
495 days. Serum was collected via cheek bleed as described above to monitor viral titer from d1pi to
496 d4pi. Mice whose body weight dropped below 80% of their initial weight were humanely
497 euthanized using CO_2 overdose followed by cervical dislocation as a secondary confirmatory
498 method. All animal experiments were approved by the Saint Louis University Institutional Animal
499 Care and Use Committee (IACUC).

500 **Statistical analysis**

501 GraphPad Prism version 9.0 was used for statistical analysis. Titer and % infection of D2-
502 vFLM were compared to the DV2 using two-way ANOVA. EC_{50} and $FRNT_{50}$ were compared using
503 Student's t-test. Significant symbols are as follows: *, $P < 0.05$; **, $P< 0.005$; ***, $P < 0.0005$; ****,
504 $P < 0.00005$. The data are graphed as means ± standard deviations. All experiments were
505 conducted at least three times, except for experiments involving serum were performed at least
506 2 times due to limited regents.

507

508 **ACKNOWLEDGEMENTS**

509 We thank members of the Tse laboratory for helpful discussions. We also thank Department of
510 Comparative Medicine at Saint Louis University for providing guidance and help for animal
511 experiments. We also thank Dr. Eva Harris at UC Berkeley for providing the D220 mouse adaptive
512 DENV2 challenge strain. This work was supported by Saint Louis University Department of
513 Molecular Microbiology and Immunology Startup fund, SLU-SOM President's Research Award,
514 and Institute for Drug and Biotherapeutic Innovation Seed Grant.

515

516 **AUTHOR CONTRIBUTION**

517 L.V.T. designed the study. Y.R.D, J.J.A., K.D., L.J.S., and L.V.T. performed experiments. L.V.T.
518 and R.M.M. performed high-throughput sequencing preparation and analysis. provided reagents.
519 L.V.T. provided oversight of the project and funding. L.V.T. wrote the manuscript. Y.R.D., R.M.M.

and L.V.T. reviewed and revised the final version. All authors approved the final version of the manuscript.

CONFLICT DISCLOSURE

L.V.T. and R.M.M. are inventors on a patent application filed on the subject matter of the manuscript.

525 **REFERENCES**

526 1. Zhang, W.-X. *et al.* Assessing the global dengue burden: Incidence, mortality, and disability
527 trends over three decades. *PLoS Negl Trop Dis* **19**, e0012932 (2025).
528 2. World Health Organization. Disease Outbreak News; Dengue – Global Situation.
529 https://www.who.int/emergencies/disease-outbreak-news/item/2024-DON518 (2024).
530 3. Guzman, M. G. & Harris, E. Dengue. *Lancet* **385**, 453–465 (2015).
531 4. Screaton, G., Mongkolsapaya, J., Yacoub, S. & Roberts, C. New insights into the
532 immunopathology and control of dengue virus infection. *Nat Rev Immunol* **15**, 745–759
533 (2015).
534 5. Halstead, S. B. Dengue Antibody-Dependent Enhancement: Knowns and Unknowns.
535 *Microbiol Spectr* **2**, (2014).
536 6. Halstead, S. B. & O'Rourke, E. J. Antibody-enhanced dengue virus infection in primate
537 leukocytes. *Nature* **265**, 739–741 (1977).
538 7. Yamin, R. *et al.* Human FcγRIIIa activation on splenic macrophages drives dengue
539 pathogenesis in mice. *Nat Microbiol* **8**, 1468–1479 (2023).
540 8. Dowd, K. A. *et al.* prM-reactive antibodies reveal a role for partially mature virions in dengue
541 virus pathogenesis. *Proc Natl Acad Sci U S A* **120**, e2218899120 (2023).
542 9. Beltramello, M. *et al.* The human immune response to Dengue virus is dominated by highly
543 cross-reactive antibodies endowed with neutralizing and enhancing activity. *Cell Host*
544 *Microbe* **8**, 271–283 (2010).
545 10. Sridhar, S. *et al.* Effect of Dengue Serostatus on Dengue Vaccine Safety and Efficacy. *New*
546 *England Journal of Medicine* **379**, 327–340 (2018).
547 11. Tricou, V. *et al.* Long-term efficacy and safety of a tetravalent dengue vaccine (TAK-003):
548 4·5-year results from a phase 3, randomised, double-blind, placebo-controlled trial. *The*
549 *Lancet Global Health* **12**, e257–e270 (2024).
550 12. de Silva, A. Safety of Dengue Vaccine? *Clin Infect Dis* **76**, 371–372 (2023).

551 13. Kallás, E. G. *et al.* Live, Attenuated, Tetravalent Butantan–Dengue Vaccine in Children and
552 Adults. *New England Journal of Medicine* **390**, 397–408 (2024).
553 14. Lai, C.-Y. *et al.* Antibodies to Envelope Glycoprotein of Dengue Virus during the Natural
554 Course of Infection Are Predominantly Cross-Reactive and Recognize Epitopes Containing
555 Highly Conserved Residues at the Fusion Loop of Domain II. *J Virol* **82**, 6631–6643 (2008).
556 15. Wollner, C. J. *et al.* A Dengue Virus Serotype 1 mRNA-LNP Vaccine Elicits Protective
557 Immune Responses. *J Virol* **95**, e02482-20.
558 16. Collins, N. D. & Barrett, A. D. T. Live Attenuated Yellow Fever 17D Vaccine: A Legacy
559 Vaccine Still Controlling Outbreaks In Modern Day. *Curr Infect Dis Rep* **19**, 14 (2017).
560 17. Lee, M. F., Long, C. M. & Poh, C. L. Current status of the development of dengue vaccines.
561 *Vaccine: X* **22**, 100604 (2025).
562 18. Whitehead, S. S. Development of TV003/TV005, a single dose, highly immunogenic live
563 attenuated dengue vaccine; what makes this vaccine different from the Sanofi-Pasteur
564 CYD™ vaccine? *Expert Rev Vaccines* **15**, 509–517 (2016).
565 19. Meganck, R. M. *et al.* Evolution of a functionally intact but antigenically distinct DENV fusion
566 loop. *eLife* **12**, RP87555 (2023).
567 20. Kiesslich, S. & Kamen, A. A. Vero cell upstream bioprocess development for the production
568 of viral vectors and vaccines. *Biotechnology Advances* **44**, 107608 (2020).
569 21. Haughney, S. *et al.* Optimization for the production of a dengue live-attenuated Quadrivalent
570 vaccine in Vero cells grown on microcarriers. *Vaccine: X* **24**, 100658 (2025).
571 22. Tse, L. V. *et al.* Generation of Mature DENVs via Genetic Modification and Directed
572 Evolution. *mBio* **13**, e00386-22 (2022).
573 23. Kotaki, T. *et al.* An affinity-matured human monoclonal antibody targeting fusion loop epitope
574 of dengue virus with in vivo therapeutic potency. *Sci Rep* **11**, 12987 (2021).

575 24. Aklil, Y. *et al.* Development of a novel plate reader-based antibody-dependent enhancement
576 (ADE) assay for orthoflavivirus infections. *Journal of Virological Methods* **338**, 115210
577 (2025).
578 25. Chelluboina, S. *et al.* Evaluation of methods for the measurement of antibody-dependent
579 enhancement of dengue virus infection using different FcγRIIa expressing cell lines. *PLOS*
580 *ONE* **20**, e0331320 (2025).
581 26. Orozco, S. *et al.* Characterization of a model of lethal dengue virus 2 infection in C57BL/6
582 mice deficient in the alpha/beta interferon receptor. *J Gen Virol* **93**, 2152–2157 (2012).
583 27. Wang, Y. *et al.* Rational design of flavivirus E protein vaccine optimizes immunogenicity and
584 mitigates antibody dependent enhancement risk. *Nat Commun* **16**, 11558 (2025).
585 28. Thiono, D. J. *et al.* Stabilized dengue virus 2 envelope subunit vaccine redirects the
586 neutralizing antibody response to all E-domains. *Journal of Virology* **99**, e00229-25 (2025).
587 29. Lien, S.-B. *et al.* A novel immunogen comprising a bc loop and mutant fusion loop epitopes
588 generates potent neutralization and protective abilities against flaviviruses without risk of
589 disease enhancement. *Vaccine* **57**, 127219 (2025).
590 30. Tan, B. E. K., Tham, S. K. & Poh, C. L. Development of New Live-Attenuated Vaccine
591 Candidates Lacking Antibody-Dependent Enhancement (ADE) Against Dengue. *Vaccines*
592 **13**, (2025).
593 31. Tian, Y., Grifoni, A., Sette, A. & Weiskopf, D. Human T Cell Response to Dengue Virus
594 Infection. *Front. Immunol.* **10**, (2019).
595 32. Weiskopf, D. *et al.* The Human CD8+ T Cell Responses Induced by a Live Attenuated
596 Tetravalent Dengue Vaccine Are Directed against Highly Conserved Epitopes. *Journal of*
597 *Virology* **89**, 120–128 (2014).
598 33. Degrève, L., Fuzo, C. A. & Caliri, A. Extensive structural change of the envelope protein of
599 dengue virus induced by a tuned ionic strength: conformational and energetic analyses. *J*
600 *Comput Aided Mol Des* **26**, 1311–1325 (2012).

601 34. Zhang, Y. *et al.* Conformational Changes of the Flavivirus E Glycoprotein. *Structure* **12**,
602 1607–1618 (2004).
603 35. Hein, L. D. *et al.* Multiplex sample-sparing assay for detecting type-specific antibodies to
604 Zika and dengue viruses: an assay development and validation study. *Lancet Microbe* **6**,
605 100951 (2025).
606 36. Henein, S. *et al.* Dengue vaccine breakthrough infections reveal properties of neutralizing
607 antibodies linked to protection. *J Clin Invest* **131**, e147066, 147066 (2021).
608 37. Henein, S. *et al.* Dissecting Antibodies Induced by a Chimeric Yellow Fever-Dengue, Live-
609 Attenuated, Tetravalent Dengue Vaccine (CYD-TDV) in Naive and Dengue-Exposed
610 Individuals. *J Infect Dis* **215**, 351–358 (2017).
611 38. Bournazos, S., Gupta, A. & Ravetch, J. V. The role of IgG Fc receptors in antibody-
612 dependent enhancement. *Nat Rev Immunol* **20**, 633–643 (2020).
613 39. Sharma, A. *et al.* The epitope arrangement on flavivirus particles contributes to Mab C10's
614 extraordinary neutralization breadth across Zika and dengue viruses. *Cell* **184**, 6052-
615 6066.e18 (2021).
616 40. Gallichotte, E. N. *et al.* Vaccine-induced antibodies to contemporary strains of dengue virus
617 type 4 show a mechanistic correlate of protective immunity. *Cell Reports* **39**, (2022).
618 41. Martinez, D. R. *et al.* Antigenic Variation of the Dengue Virus 2 Genotypes Impacts the
619 Neutralization Activity of Human Antibodies in Vaccinees. *Cell Reports* **33**, 108226 (2020).
620 42. Rouvinski, A. *et al.* Covalently linked dengue virus envelope glycoprotein dimers reduce
621 exposure of the immunodominant fusion loop epitope. *Nat Commun* **8**, 15411 (2017).
622 43. Fang, E. *et al.* Construction of a Dengue NanoLuc Reporter Virus for In Vivo Live Imaging in
623 Mice. *Viruses* **14**, 1253 (2022).
624 44. Routh, A., Head, S. R., Ordoukhanian, P. & Johnson, J. E. ClickSeq: Fragmentation-free
625 next-generation sequencing via click-ligation of adaptors to stochastically terminated 3'-
626 azido cDNAs. *J Mol Biol* **427**, 2610–2616 (2015).

629 **Figure Legends**

630 **Figure 1.** Adaptation and characterization of D2-vFLM D2-FLM. **A)** Immunofluorescent staining
631 of DV2 and D2-FLM infected Vero-81 cells with a-NS3 antibody at 24 hours post-infection. **B)**
632 Combined staining of prM and E of DV-2 and D2-FLM infected Vero-81 cells at 32°C and 37°C at
633 5 days post-infection. **C)** Schematic of D2-vFLM mammalian cell adaptation. Multiple-step growth
634 curves of DV2, D2-FLM, and D2-vFLM in **D)** Vero-81 and **E)** C6/36 cells. **F)** Western blot of DV2
635 and D2-vFLM with a-E and a-prM antibodies. Right: over-exposure to visualize prM in D2-vFLM.
636 **G)** Quantification of prM:E ratio of D2-vFLM, normalized to DV2. Growth curves were analyzed
637 by multiple t-test comparison
638 between DV2 and D2-vFLM
639 at different time points.
640 Western blot quantification
641 was analyzed by Students *t*-
642 test.

643

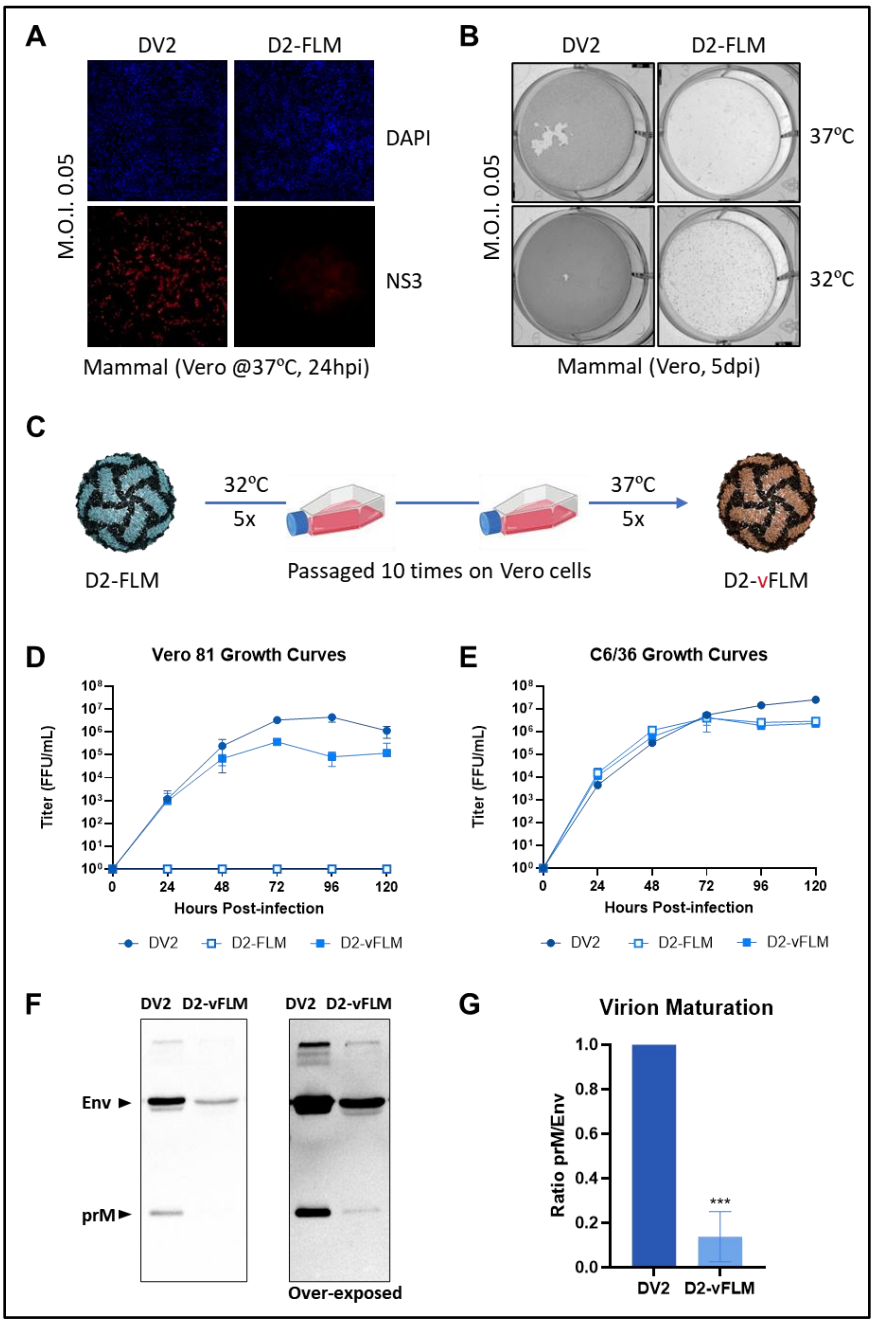

644 **Figure S1.** Temperature and pH stability of DV2 and D2-vFLM assessed using a nLuc reporter
645 assay. **A)** Infectivity of DV2-nLuc and D2-vFLM-nLuc following incubation at temperatures ranging
646 from 4°C to 55°C, normalized to the control 4°C condition. **B)** Infectivity of DV2-nLuc and D2-
647 vFLM-nLuc following exposure to buffers at pH 8.4, 7.4, 6.4, or 5.4, normalized to the untreated
648 control. Statistics were performed by Students *t*-test.

649

650

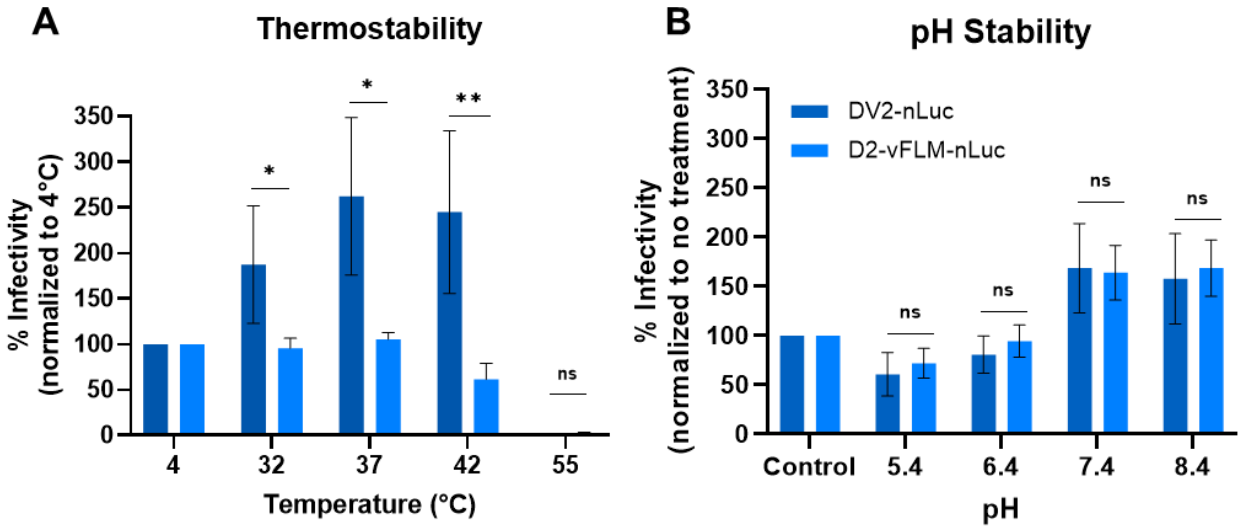

651 **Table 1.** Engineered and acquired mutations for different D2-vFLM mutants in Vero-81 cells.

	D2-vFLM	D2-vFLM-strucutral	D2-vFLM-nonstructural
Structural mutations			
prM-E18D	100%	100% (I)	-
prM-L41V	-	-	*100% (A)*
Env-P53T	100%	100% (I)	-
Env-T171A	100%	100% (I)	*95.4% (A)*
Env-K204R	100%	100% (I)	-
Env-T404K	-	-	*97.3% (A)*
Nonstructural mutations			
NS2A-L181F	100%	-	100% (I)
N24b-L112F	100%	-	100% (I)
NS1-M89V	-	*31% (A)*	-
NS3-D409E	-	*14% (A)*	-
NS4b-V115A	-	*13% (A)*	-

(I): Intended mutations; *(A): Acquired mutations*; - Not Applicable

652 **Figure 2.** Compensatory mutations in structural proteins are important for Vero-81 adaptation. **A)**
653 Virus yield of D2-vFLM-strucutral and -nonstructural infectious clones grown on C6/36 cells.
654 Multiple-cycle growth curves of **B)** Vero grown or **C)** C6/36 grown virus D2-vFLM-strucutral and -
655 nonstructural viruses on Vero-81 cells.
656

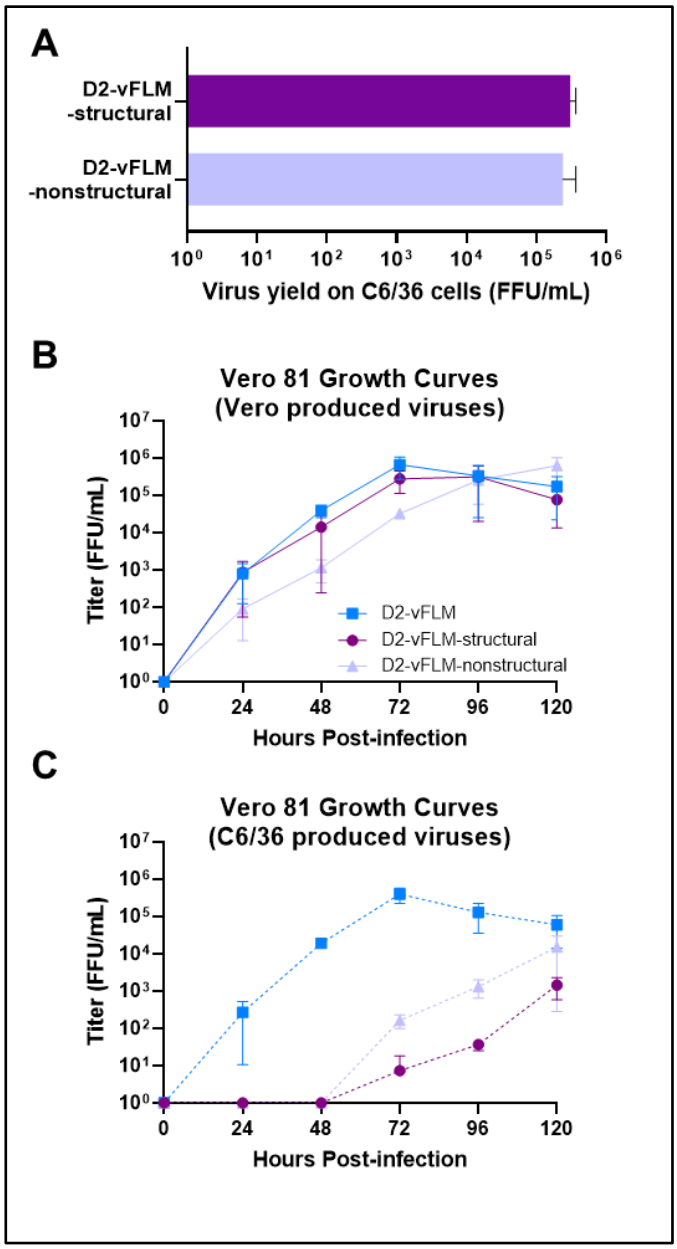

657 **Figure 3.** Grafting and adaptation of FLM mutations on DENV4. **A)** Growth curves of DV4, D4-
658 FLM and D4-vFLM on Vero-81 cells. **B)** Acquired mutations of D4-vFLM after serial passage in
659 Vero-81 cells. **C)** Structural model of DENV-Envelope-dimer with color coded FL mutations and
660 Vero adaptation mutations from DENV2 and DENV4.

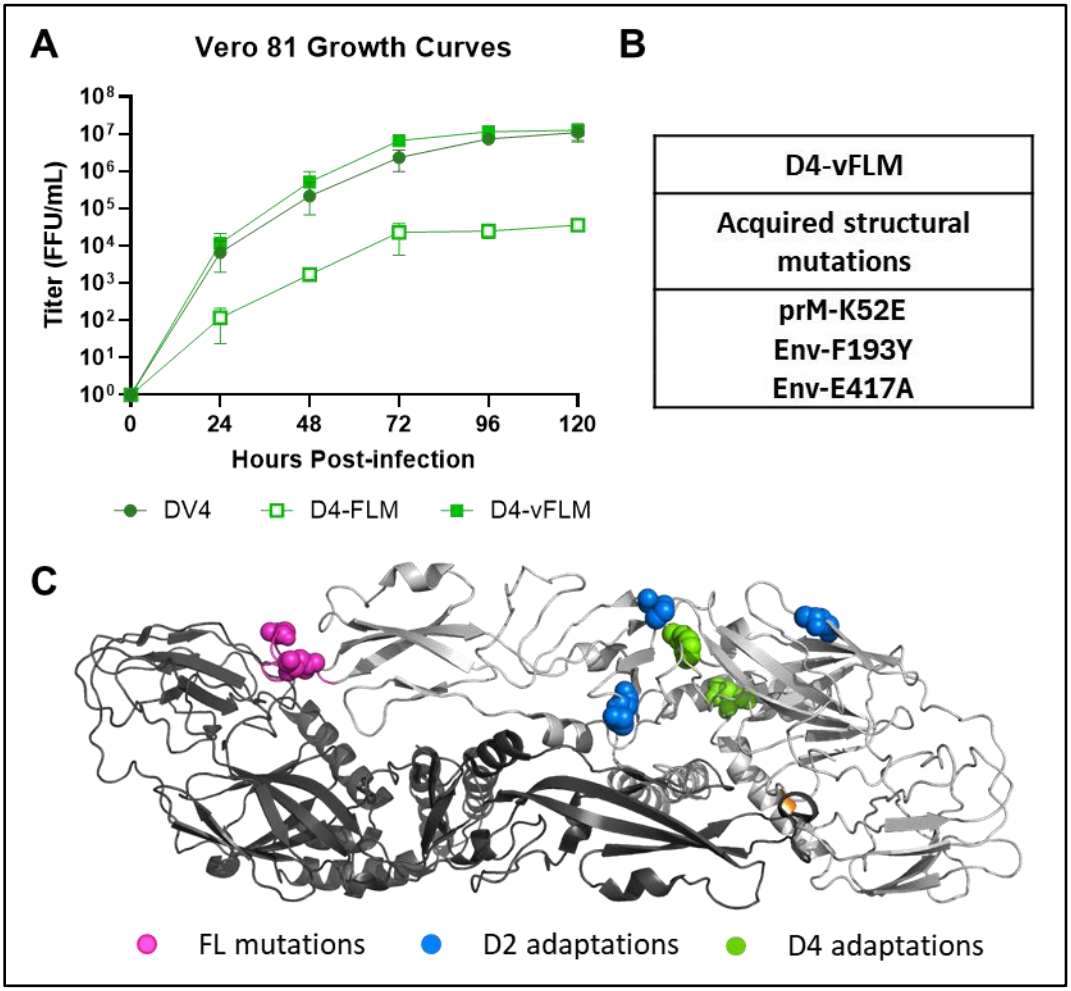

661 **Figure 4.** Antigenicity of DENV and DENV-vFLM. $FRNT_{50}$ of **(A)** DV2 and D2-vFLM or **(B)** DV4
662 and D4-vFLM against mAbs on Vero-81 cells. EC_{50} of **(C)** DV2-nLuc and D2-vFLM-nLuc or **(D)**
663 DV4-nLuc and D4-vFLM-nLuc against mAbs on Vero-81 cells. Statistics were performed by
664 Students *t*-test.

665

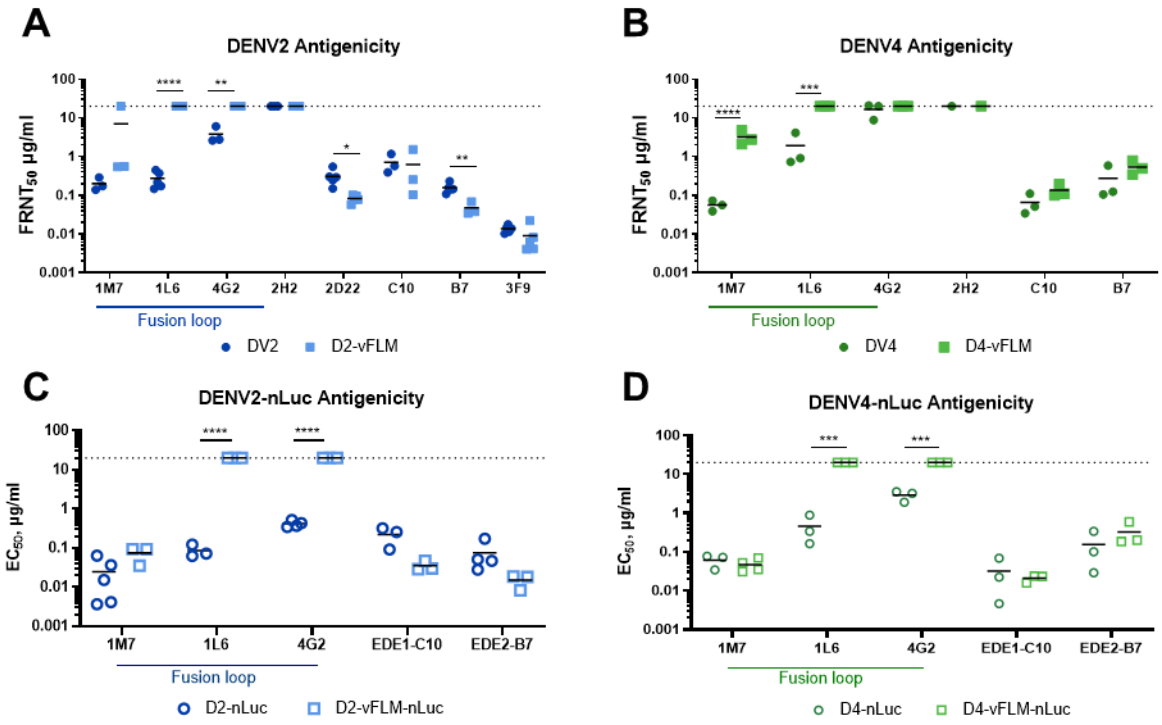

666 **Figure 5.** Immunogenicity of DVs and D2-vFLMs *in vivo*. **A)** Homotypic (against DV2-nLuc) and
667 heterotypic (against DV4-nLuc) EC_{50} of pooled serum of DV2 and D2-vFLM from pre-
668 immunization, 2wk after prime, 2wk after 1°boost, and 2 wk after 2°boost. **B)** Homotypic and
669 heterotypic EC_{50} of individual DV2 and D2-vFLM serum from immunized C57BL/6 mice after
670 2°Boost. EC_{50} of pooled serum were analyzed by two-way ANOVA with multiple comparisons
671 compared to pre-immunization. Mean EC_{50} of the 2°boost was compared by Students *t*-test.

672

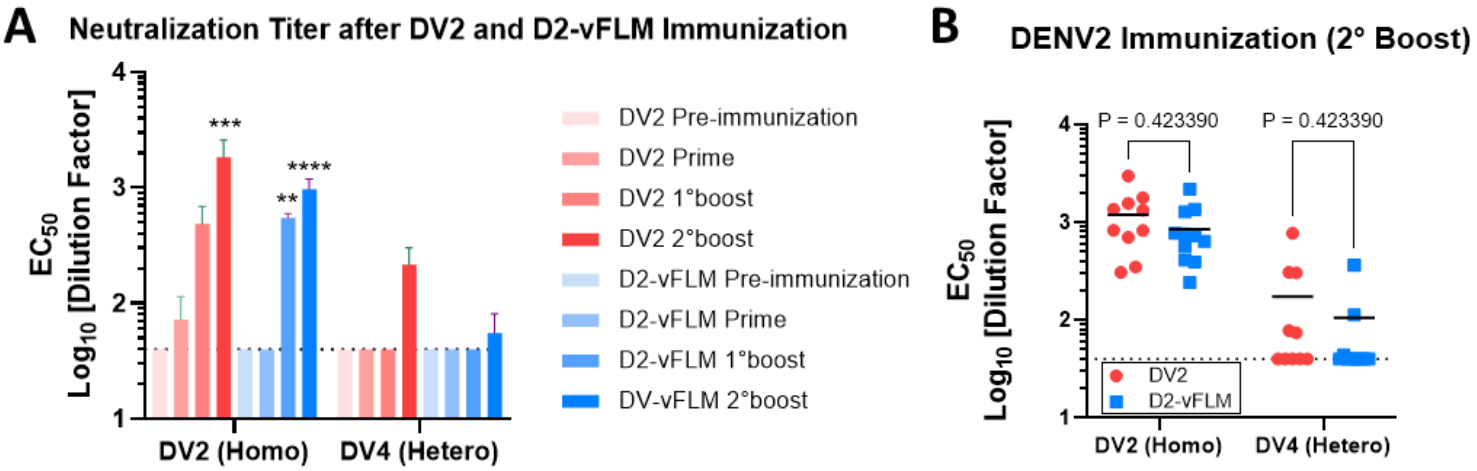

673 **Figure. S2.** Neutralization curves of pooled serum samples from **A)** DV2 and **B)** D2-vFLM
674 immunized mice against homotypic and heterotypic DENV-nLuc.

675

676

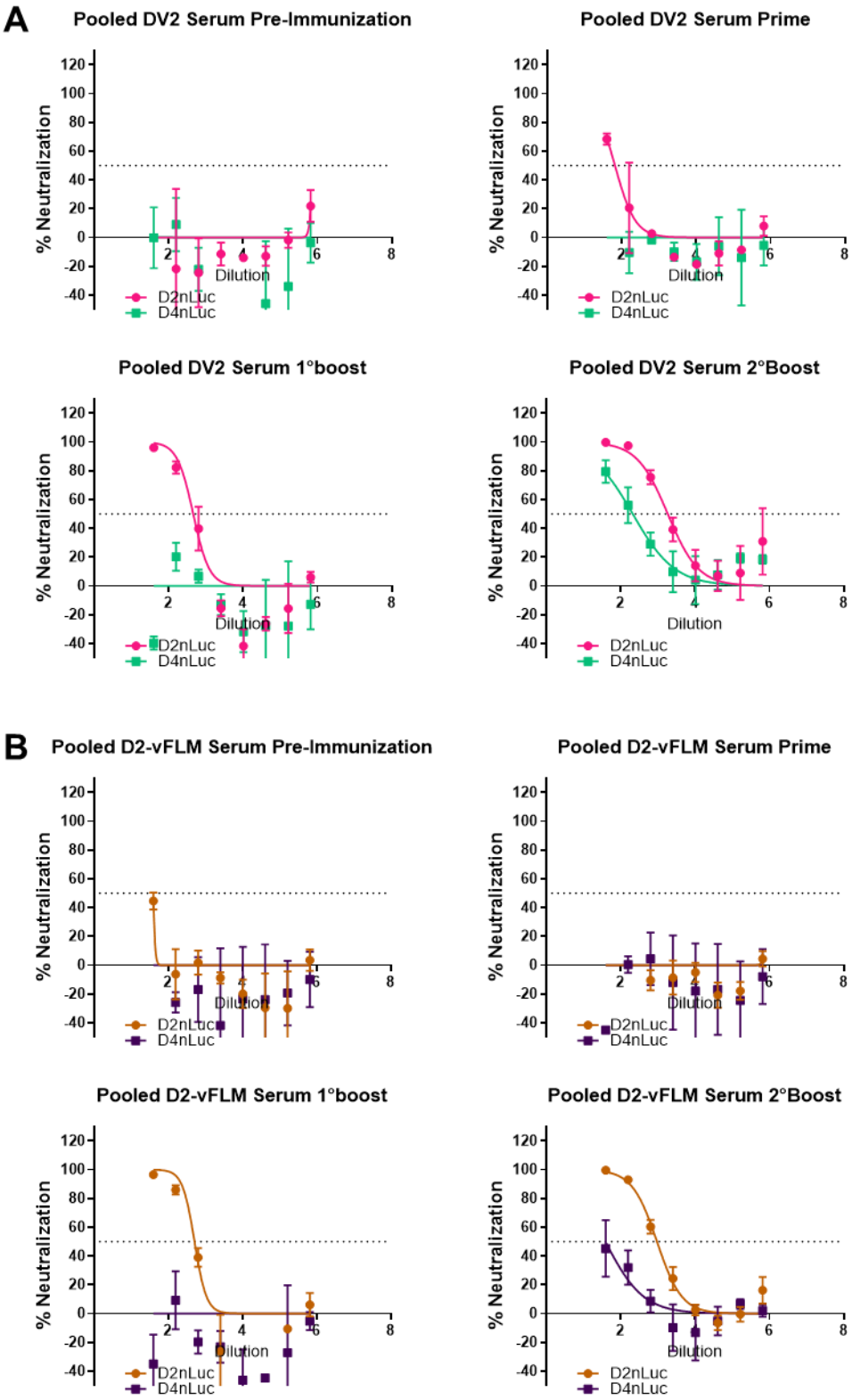

677 **Figure S3.** Individual neutralization curves of **A)** DV2 and **B)** D2-vFLM serum after 2°boost
678 against homotypic (DV2-nLuc) and heterotypic (DV4-nLuc).

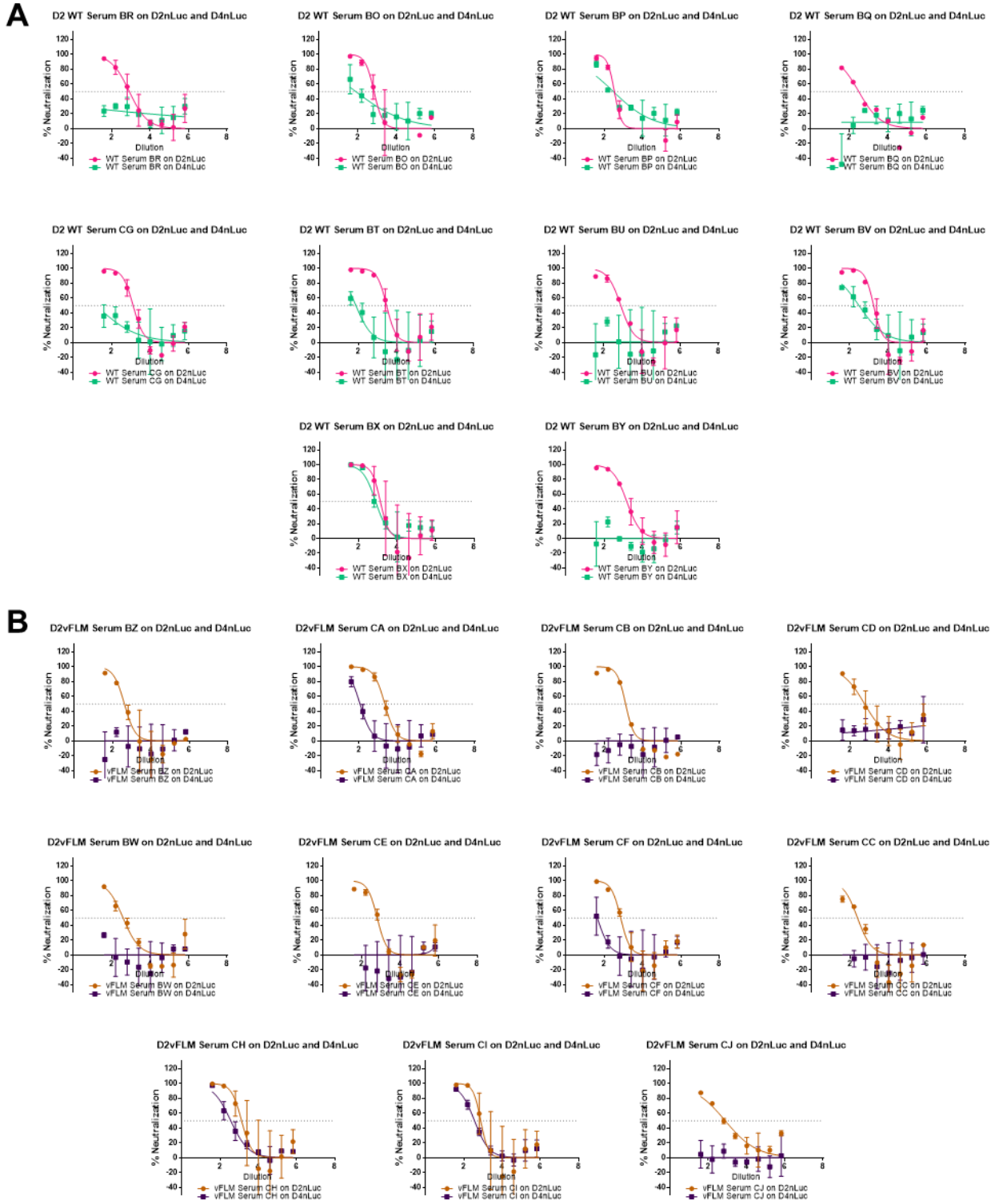

679 **Figure 6.** High-throughput nLuc-based ADE assay shows no heterotypic ADE from serum isolated
680 from D2-vFLM immunized mice. Monoclonal Ab control and fold-increase in infectivity of DV4-
681 nLuc and D4-vFLM-nLuc against **A)** 4G2, **B)** 2H2, and **C)** B7 in K562 cells. **D)** Heterotypic ADE
682 against pooled serum from DV2 and D2-vFLM immunized mice that are positive against DV4.
683 Error bars denote ±1 S.D. Data was analyzed by two-way ANOVA; statistical significance shown
684 corresponds to the interaction between groups.
685

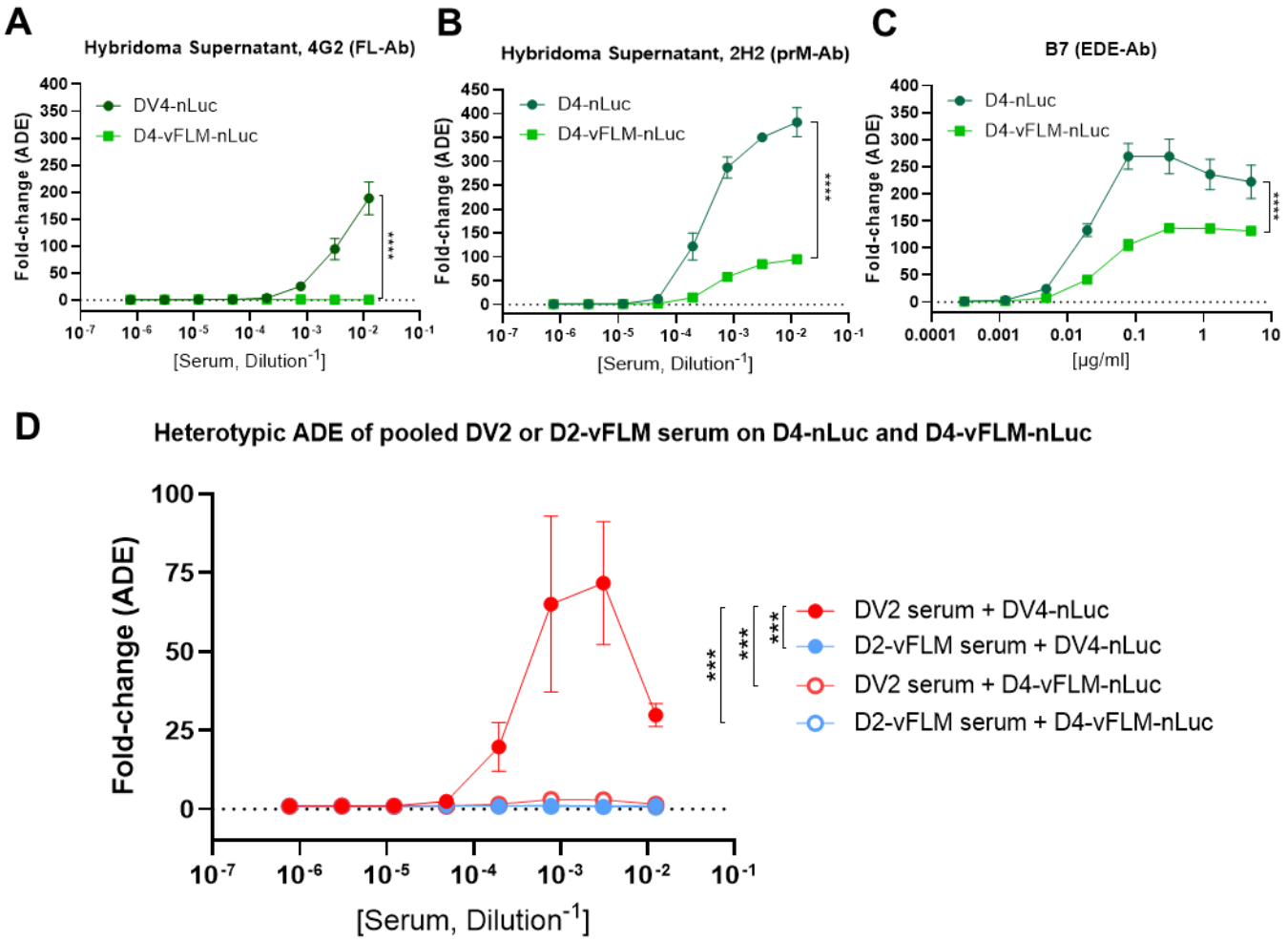

686 **Figure S4.** Individual heterotypic ADE curves of DV4-nLuc and D4-vFLM-nLuc against DV2 and
687 D2-vFLM serum from immunized mice. Vertical dotted lines denote the EC50 of the serum against
688 DV4-nLuc.

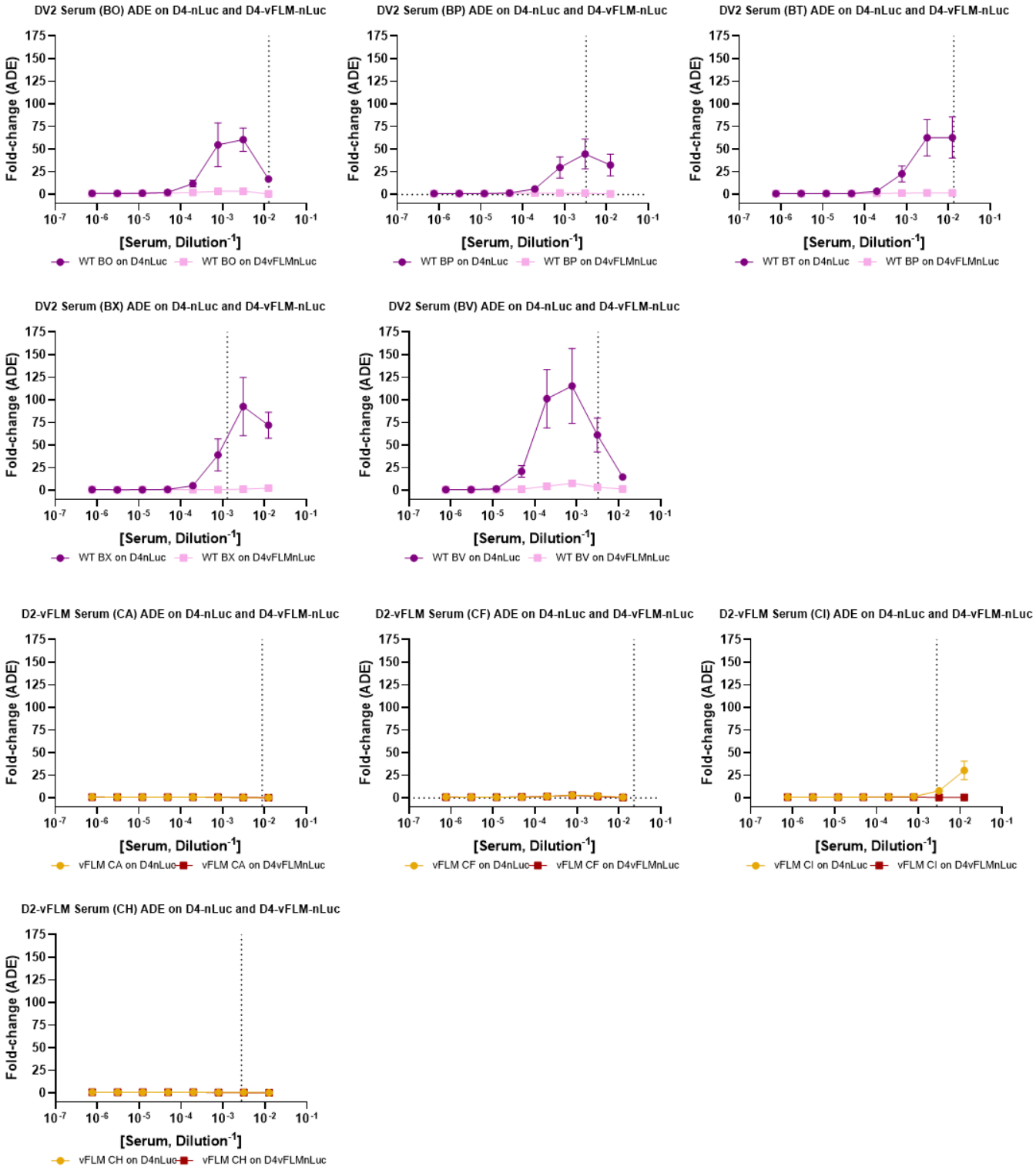

689 **Figure 7.** D2-vFLM immunization protects AG129 mice from lethal challenge. AG129 mice were
690 immunized with DV2 (n=4), D2-vFLM (n=5), or mock (n=6) immunized and challenged with D220
691 virus. **A)** Percent weight loss, analyzed by linear mixed-effects model with repeated measures.
692 Pairwise group comparisons were performed using estimated marginal means with Tukey
693 adjustment. **B)** Survival curves up to 10 days
694 post challenge, assessed with Log-rank
695 (Mantel–Cox) test, and pairwise comparisons
696 performed with Bonferroni correction for
697 multiple testing. **C)** Serum viral titer from d1pi
698 - d4pi. Individual mice are only bled twice per
699 week for humane treatment. $p < 0.05$ was
700 considered statistically significant. Θ
701 represents unexpected mouse death on d1pi
702 in the DV2 immunization group.

703

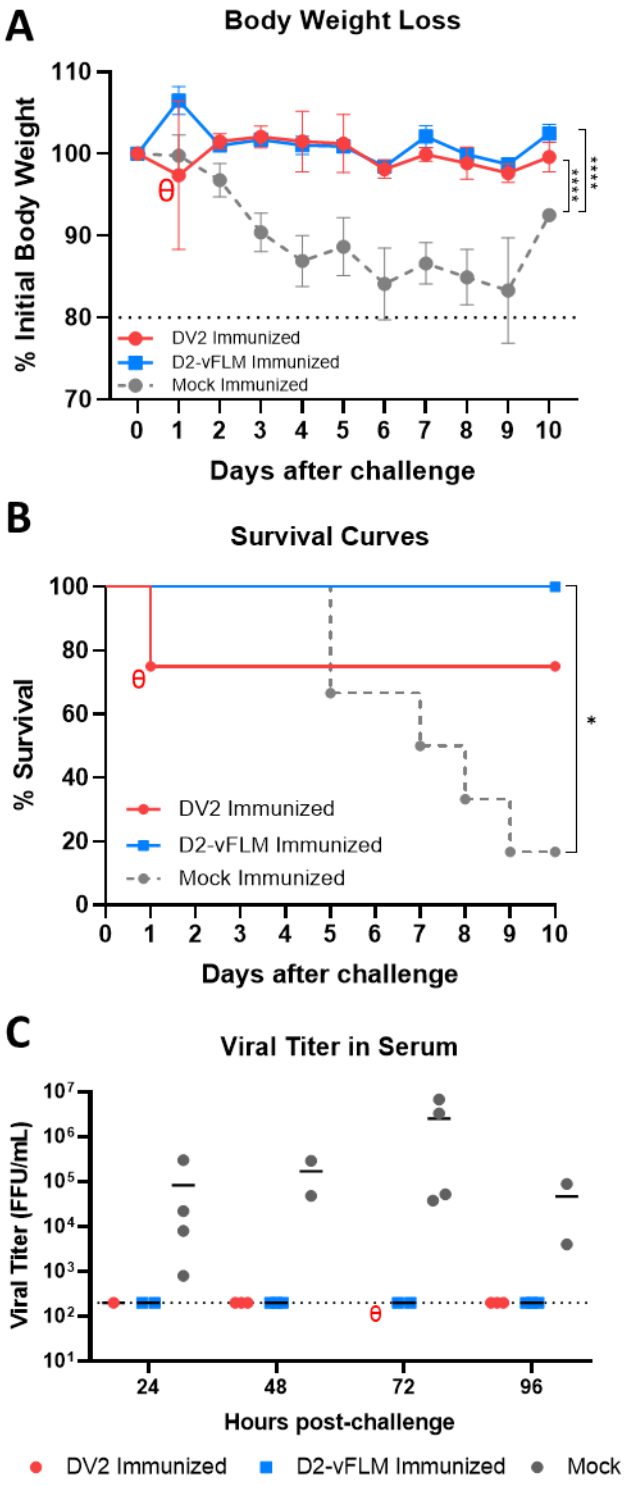

Fusion Loop Modified and Mature Dengue Virus Elicits Protective Serum with Minimal Antibody Dependent Enhancement

Yago R. Dalben[1], Jacob J. Adler[1], Rita M. Meganck[2], Katelyn Duenas[3], Lisa J. Snoderly-Foster[1], Longping V. Tse[1]

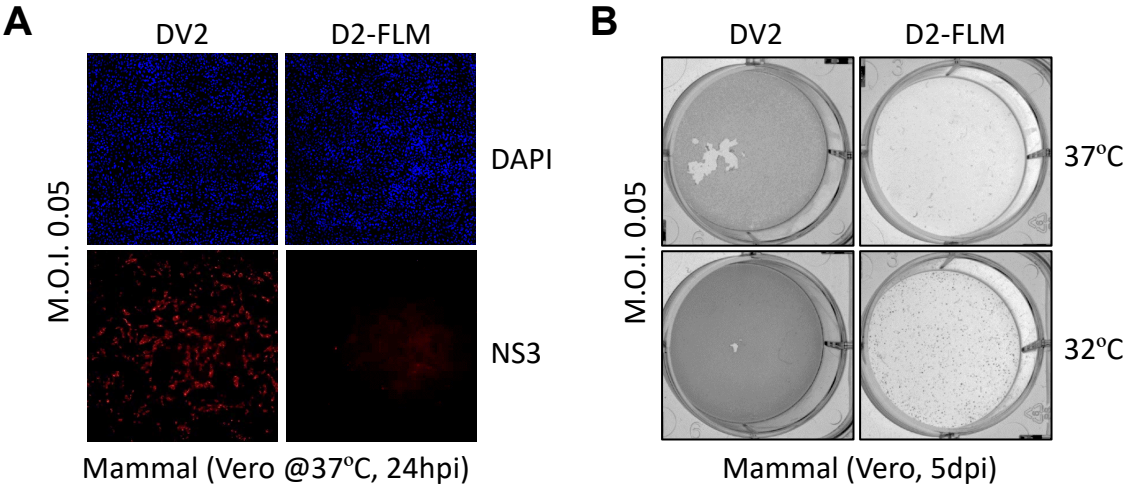
A
DV2
D2-FLM
M.O.I. 0.05
DAPI
NS3
Mammal (Vero @37°C, 24hpi)
B
DV2
D2-FLM
M.O.I. 0.05
37°C
32°C
Mammal (Vero, 5dpi)

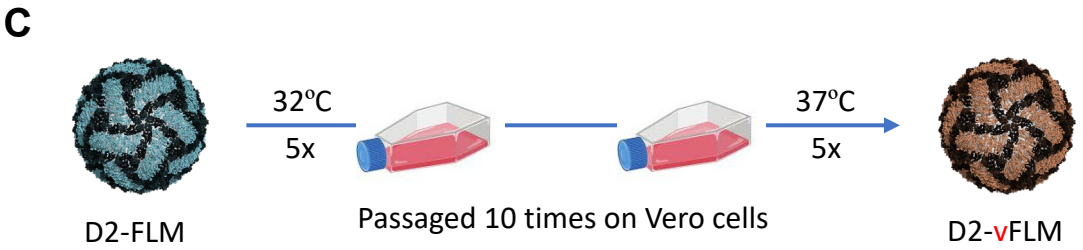
C
32°C
5x
37°C
5x
D2-FLM
Passaged 10 times on Vero cells
D2-vFLM

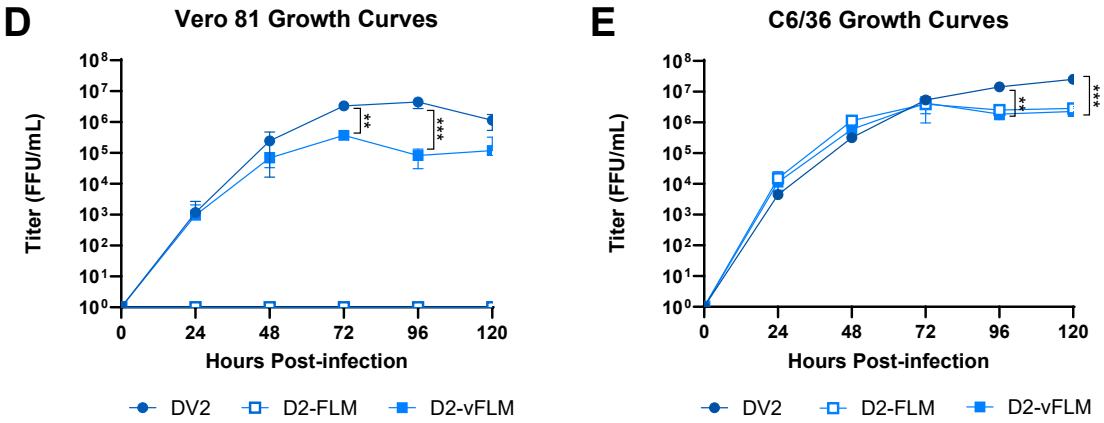
D
Vero 81 Growth Curves
Titer (FFU/mL)
Hours Post-infection
DV2
D2-FLM
D2-vFLM
E
C6/36 Growth Curves
Titer (FFU/mL)
Hours Post-infection
DV2
D2-FLM
D2-vFLM

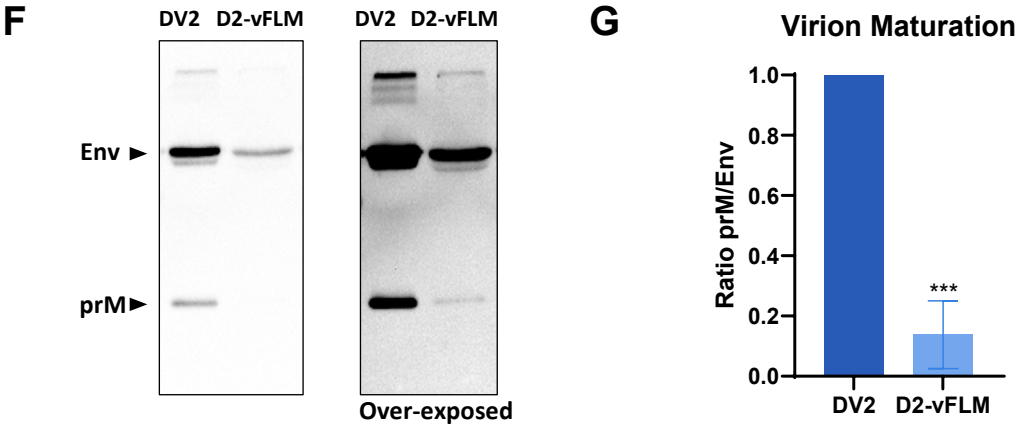
F
DV2 D2-vFLM
DV2 D2-vFLM
Env
prM
Over-exposed
G
Virion Maturation
Ratio prM/Env
DV2
D2-vFLM

Table 1. Intended and acquired mutations for different D2-vFLM mutants in Vero 81 cells

	D2-vFLM	D2-vFLM-strucutral	D2-vFLM-nonstructural
Structural mutations			
prM-E18D	100%	100% (I)	-
prM-L41V	-	-	*100% (A)*
Env-P53T	100%	100% (I)	-
Env-T171A	100%	100% (I)	*95.4% (A)*
Env-K204R	100%	100% (I)	-
Env-T404K	-	-	*97.3% (A)*
Nonstructural mutations			
NS2A-L181F	100%	-	100% (I)
N24b-L112F	100%	-	100% (I)
NS1-M89V	-	*31% (A)*	-
NS3-D409E	-	*14% (A)*	-
NS4b-V115A	-	*13% (A)*	-

(I): Intended mutations; *(A): Acquired mutations*; - Not Applicable

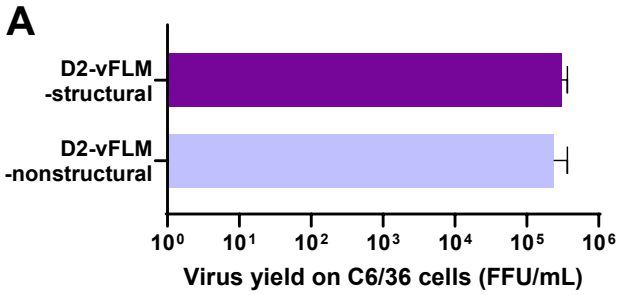
A
D2-vFLM
-structural
D2-vFLM
-nonstructural
10^0
10^1
10^2
10^3
10^4
10^5
10^6
Virus yield on C6/36 cells (FFU/mL)

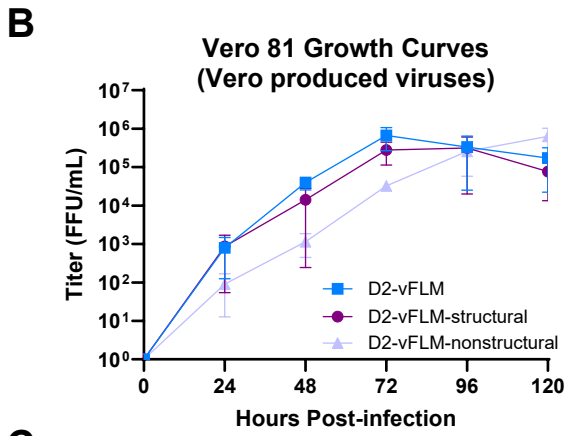
B
Vero 81 Growth Curves
(Vero produced viruses)
Titer (FFU/mL)
10^7
10^6
10^5
10^4
10^3
10^2
10^1
10^0
D2-vFLM
D2-vFLM-structural
D2-vFLM-nonstructural
0
24
48
72
96
120
Hours Post-infection

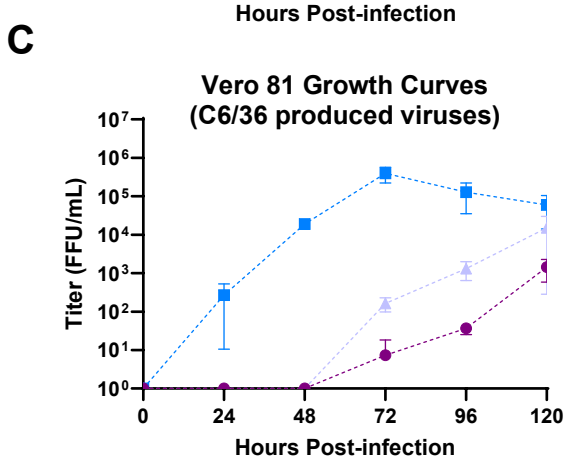
C
Vero 81 Growth Curves
(C6/36 produced viruses)
Titer (FFU/mL)
10^7
10^6
10^5
10^4
10^3
10^2
10^1
10^0
0
24
48
72
96
120
Hours Post-infection

A

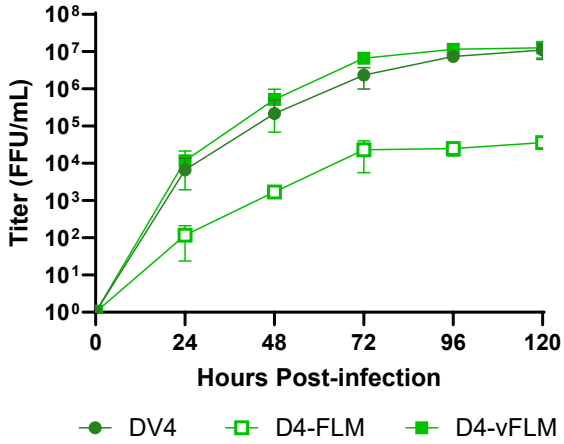

B

D4-vFLM
Acquired structural mutations
prM-K52E Env-F193Y Env-E417A

C

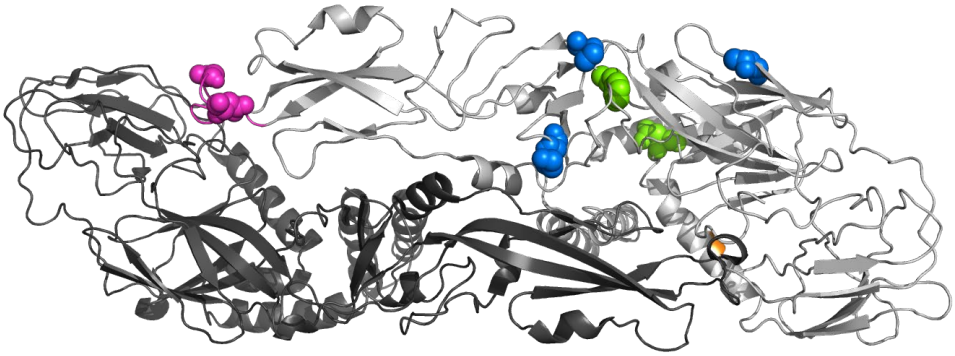

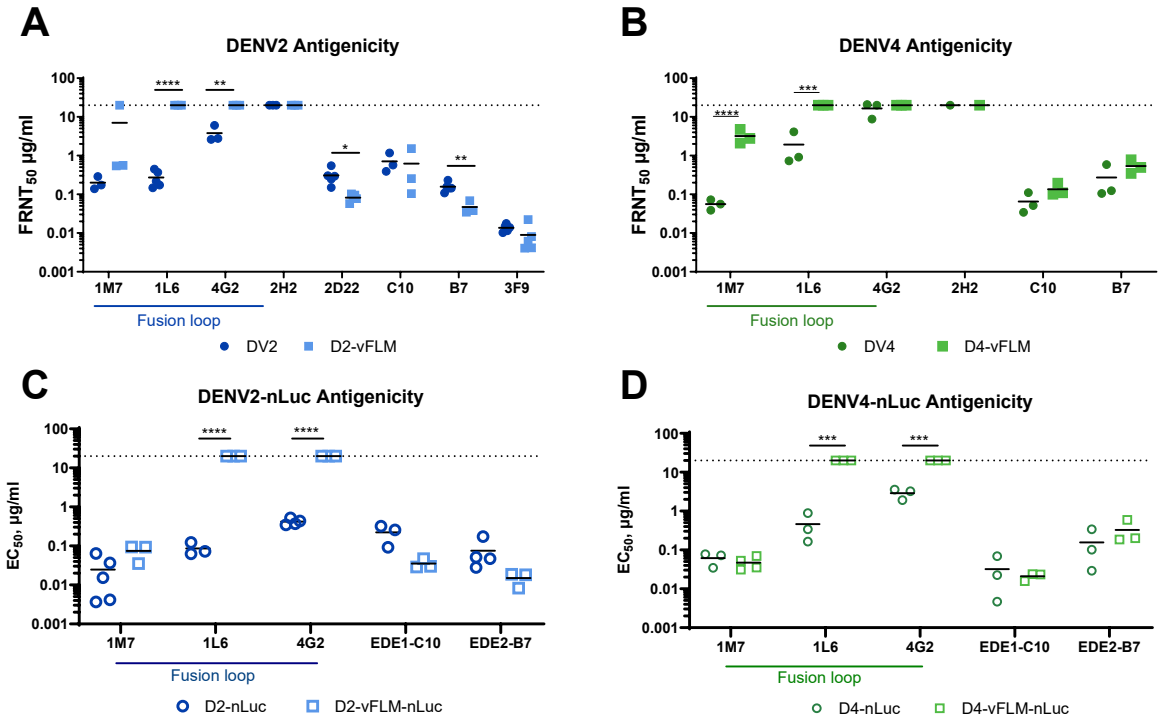
A
DENV2 Antigenicity
FRNT50 µg/ml
100
10
1
0.1
0.01
0.001
****
**
*
**
1M7
1L6
4G2
2H2
2D22
C10
B7
3F9
Fusion loop
DV2
D2-vFLM
B
DENV4 Antigenicity
FRNT50 µg/ml
****
***
1M7
1L6
4G2
2H2
C10
B7
Fusion loop
DV4
D4-vFLM
C
DENV2-nLuc Antigenicity
EC50, µg/ml
****
****
1M7
1L6
4G2
EDE1-C10
EDE2-B7
Fusion loop
D2-nLuc
D2-vFLM-nLuc
D
DENV4-nLuc Antigenicity
EC50, µg/ml
***
***
1M7
1L6
4G2
EDE1-C10
EDE2-B7
Fusion loop
D4-nLuc
D4-vFLM-nLuc

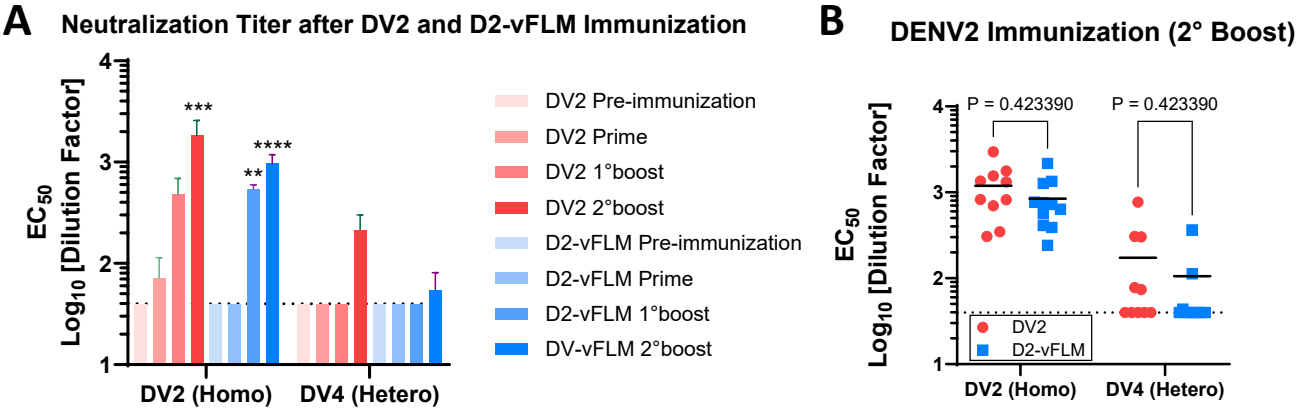
A
Neutralization Titer after DV2 and D2-vFLM Immunization
EC50
Log10 [Dilution Factor]
4
3
2
1
***
**
****
DV2 (Homo)
DV4 (Hetero)
DV2 Pre-immunization
DV2 Prime
DV2 1°boost
DV2 2°boost
D2-vFLM Pre-immunization
D2-vFLM Prime
D2-vFLM 1°boost
DV-vFLM 2°boost
B
DENV2 Immunization (2° Boost)
EC50
Log10 [Dilution Factor]
P = 0.423390
P = 0.423390
DV2
D2-vFLM
DV2 (Homo)
DV4 (Hetero)

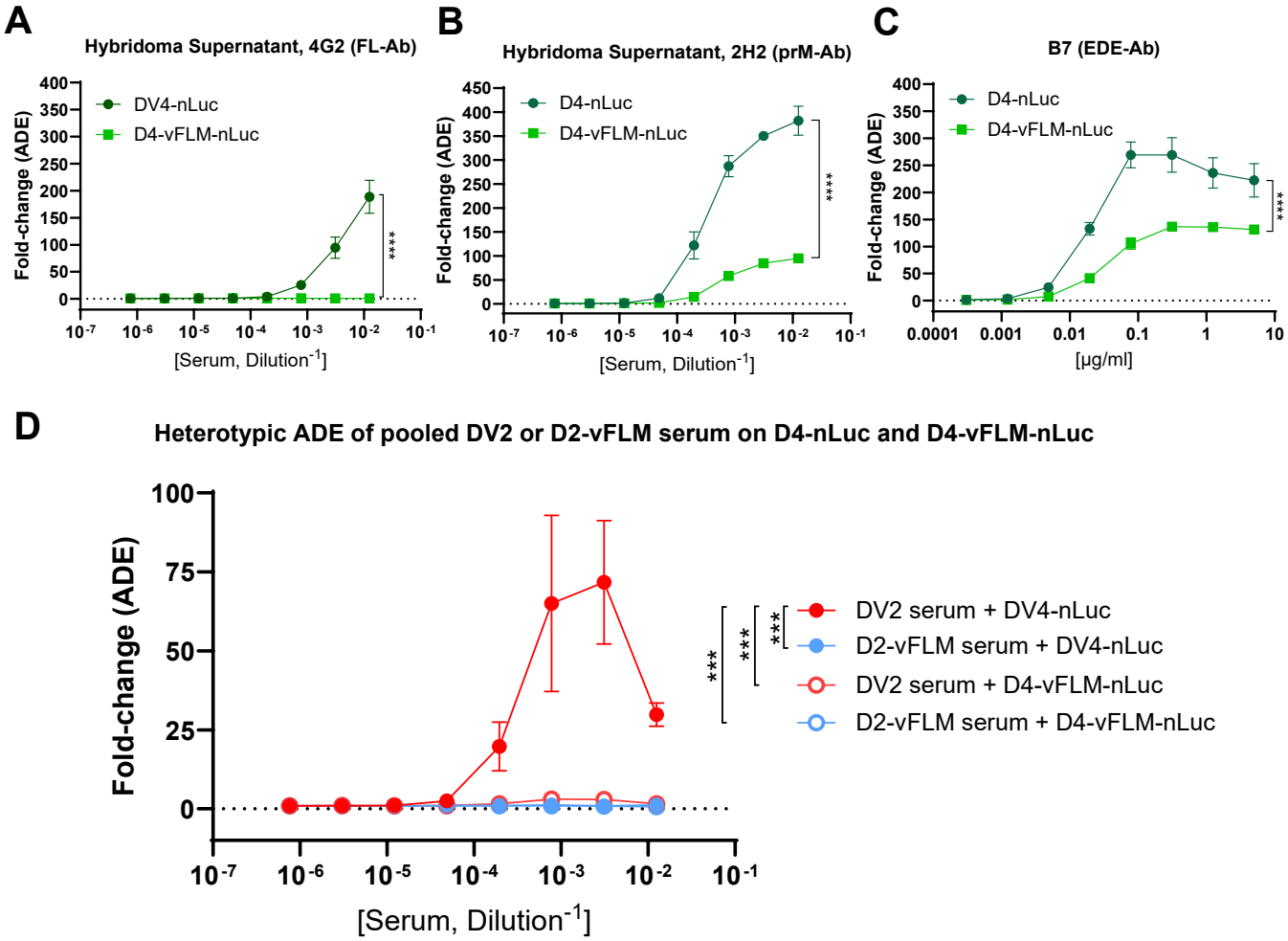
A
Hybridoma Supernatant, 4G2 (FL-Ab)
DV4-nLuc
D4-vFLM-nLuc
Fold-change (ADE)
[Serum, Dilution-1]
****
B
Hybridoma Supernatant, 2H2 (prM-Ab)
D4-nLuc
D4-vFLM-nLuc
Fold-change (ADE)
[Serum, Dilution-1]
****
C
B7 (EDE-Ab)
D4-nLuc
D4-vFLM-nLuc
Fold-change (ADE)
[μg/ml]
****
D
Heterotypic ADE of pooled DV2 or D2-vFLM serum on D4-nLuc and D4-vFLM-nLuc
Fold-change (ADE)
[Serum, Dilution-1]
***
***
***
DV2 serum + DV4-nLuc
D2-vFLM serum + DV4-nLuc
DV2 serum + D4-vFLM-nLuc
D2-vFLM serum + D4-vFLM-nLuc

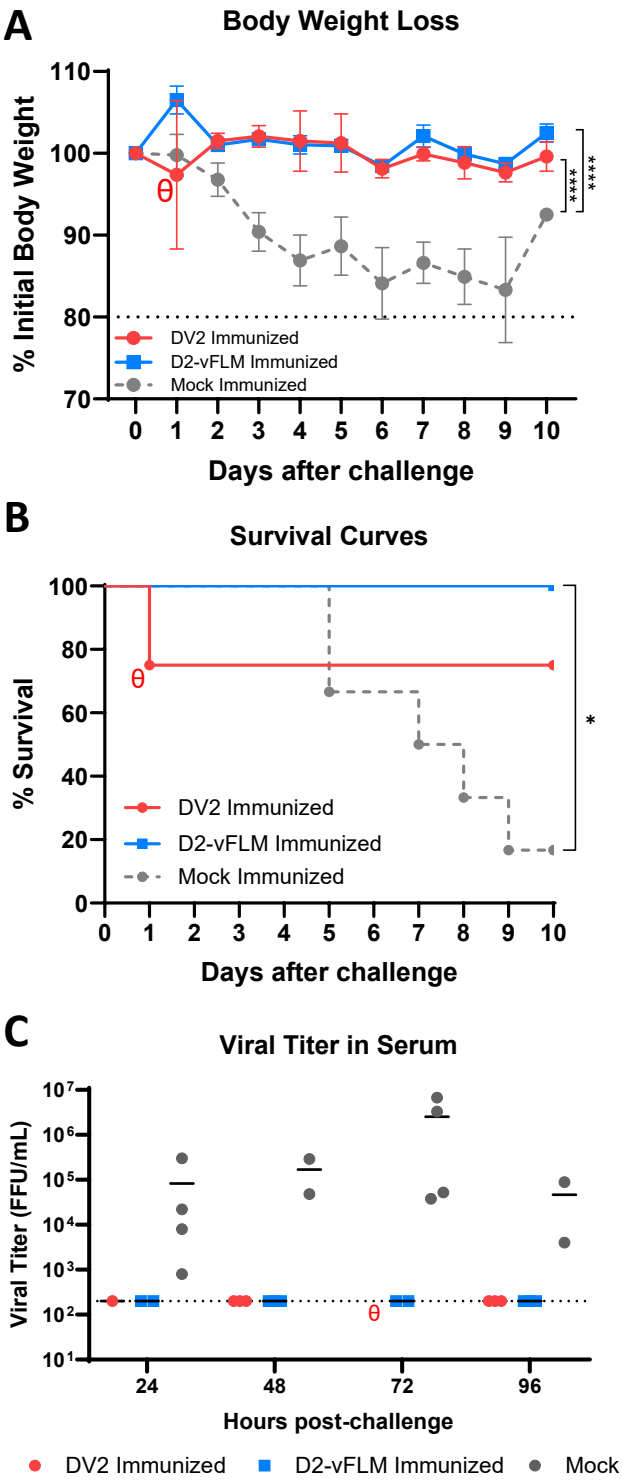
A
Body Weight Loss
% Initial Body Weight
110
100
90
80
70
θ
****
****
DV2 Immunized
D2-vFLM Immunized
Mock Immunized
0 1 2 3 4 5 6 7 8 9 10
Days after challenge
B
Survival Curves
% Survival
100
80
60
40
20
0
θ
*
DV2 Immunized
D2-vFLM Immunized
Mock Immunized
0 1 2 3 4 5 6 7 8 9 10
Days after challenge
C
Viral Titer in Serum
Viral Titer (FFU/mL)
10⁷
10⁶
10⁵
10⁴
10³
10²
10¹
θ
24 48 72 96
Hours post-challenge
DV2 Immunized
D2-vFLM Immunized
Mock